WIND-INDUCED DYNAMICS ANALYSIS OF A LARGE OBSERVATION WHEEL WITH TUNED MASS DAMPERS

JAMES (JAY) L. LAMB, PH.D.

AUGUST 23, 2016

AG&E STRUCTURAL ENGENUITY

15280 Addison Rd., Suite 310, Addison, Texas 75001
214.520.7202 www.age-se.com

WIND-INDUCED DYNAMICS ANALYSIS OF A LARGE OBSERVATION WHEEL WITH TUNED MASS DAMPERS

EXECUTIVE SUMMARY

A structural dynamics study of the wind-induced motion of a large observation wheel is performed to evaluate the influence of the Wheel's motion on critical structural member design forces and occupant comfort. Structural member design forces resulting from wind and dynamic response using worst-case storm wind pressures obtained from wind tunnel tests are lower than the forces used in the design of the structure. The occupant comfort criterion defined in ISO 2631 is satisfied for operational wind speeds. Tuned mass dampers (TMDs) incorporated into each A-Frame provide structural load mitigation and a more comfortable experience for motion-sensitive occupants. Dynamics analyses indicate that two 28.5-t TMDs reduce the A-Frame leg and spindle forces and bending moments by about 10% to 15% and reduce occupant accelerations by 15% to 35% depending upon the position on the Wheel. Traditional TMDs may not provide simultaneous structural load mitigation in storm-level winds and increased occupant comfort in operation-level winds because the estimated sway mode resonance frequency increases for the higher wind forces. The maximum TMD displacement during a worst-case storm event is expected to be 950 mm; however, further investigation by the TMD design agent is required to determine if this displacement can be accommodated within the available space

1. BACKGROUND

The Engineer Of Record (EOR) for the Observation Wheel project required structural dynamics expertise to support the various wind-induced dynamics modeling and analysis efforts required to evaluate the response of the structure with respect to strength design and passenger comfort and to facilitate information flow with the tuned mass damper (TMD) design agent. The EOR developed the baseline structural model using SAP2000 and worked with wind tunnel consultants to acquire 40 1-hour-long wind force time histories for use in the various dynamics studies. The structural models and the wind force time history files have been made available to support this study.

2. STRUCTURAL DYNAMICS MODEL

The structural model of the Wheel developed by the EOR is a very detailed model intended for the design of the primary load-carrying elements of the structure using static and quasi-static loads. The level of model detail required for this activity far exceeds that required to adequately capture the primary (low frequency) structural modes of vibration. The excess detail is only an issue for the dynamics studies because of the exceedingly long computer analysis time required to produce the time history response for a given wind force time history. The detail in the original model is reduced, but retains the essential structural dynamics characteristics of the original model. An illustration of the dynamics model and revisions are provided in Figure 1.

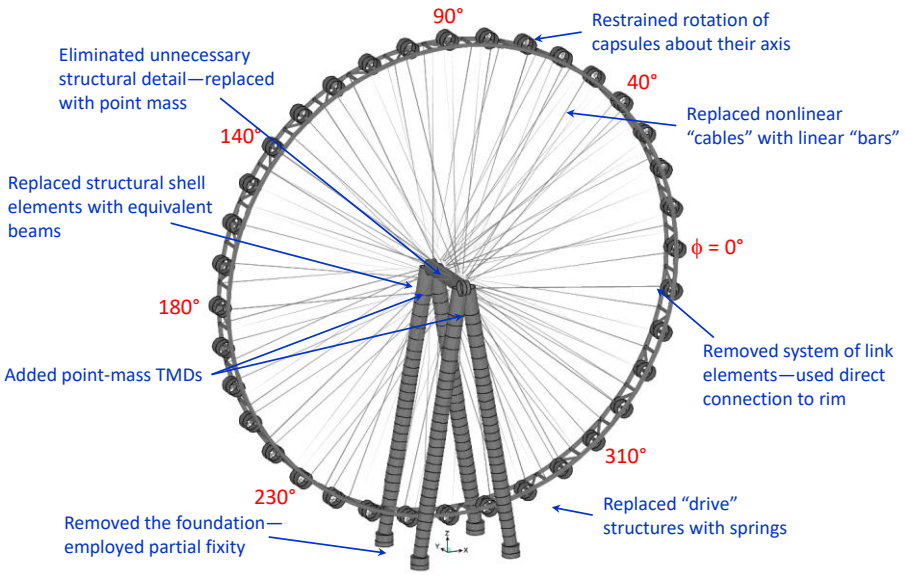

Figure 1 Linearized Dynamics Model Derived from the Detailed Nonlinear Model

The key differences between the original model and the linearized dynamics model are: the foundation elements (soil-structure interaction) and drive structures are removed from the detailed model, which includes removal of the nonlinear gap elements placed between the wheel rim and the drive structures. The internal detail and surrounding plate elements at the apex of the A-Frame and spindle are also replaced with beam elements and appropriate joint constraints that recover the stiffening effect of the outer shell. Non-critical internal structural elements are replaced with concentrated nodal masses. The nonlinear cable elements are replaced with simple beam elements with the same cross-sectional area. The end releases that allow the 36 capsule elements to rotate about their axes are fixed in the dynamics model to permit wind loads to be applied at these locations without

causing numerical instability during the numerical integration solution. Finally, point-mass models of the two TMDs are placed at the appropriate elevation in each A-Frame.

The reduction of model complexity and detail is only justified if the dynamic characteristics of the structure are retained through the simplification process. The primary modes of vibration that affect passenger comfort are below 1 Hz. The principal modes of the structure are compared for the original model (based on initial stiffness), the pre-loaded model (including a sustained lateral wind load and cable tension), and the linearized Dynamics rev0 model (corresponding to the initial stiffness model), and the linearized Dynamics rev1 model (corresponding to the pre-loaded model) in Table 1. The rev0 model is most applicable for lower wind speeds that do not "push" the Wheel against the drive structure. The rev1 model is most applicable for higher wind speeds.

Table 1 Summary and Comparison of Principal Modes

Mode	"Operating" Initial State	"Operating" Pre-Loaded	Dynamics rev0	Dynamics rev1
Rotation about Hub	0.14 Hz	0.06 Hz	0.04 Hz	0.04 Hz
1st Y-Axis Sway	0.23 Hz	0.28 Hz	0.23 Hz	0.28 Hz
Torsion about Z-Axis	0.25 Hz	0.25 Hz	0.25 Hz	0.25 Hz
Tilt about X-Axis	0.38 Hz	0.43 Hz	0.38 Hz	0.44 Hz
1st Rim Deformation	0.55 Hz	0.57 Hz	0.54 Hz	0.57 Hz
2nd Rim Deformation	0.55 Hz	0.70 Hz	0.55 Hz	0.62 Hz
1st X-Axis Sway	0.74 Hz	0.74 Hz	0.74 Hz	0.74 Hz
2nd Y-Axis Sway	0.81 Hz	0.86 Hz	0.75 Hz	0.82 Hz
3rd Rim Deformation	1.02 Hz	0.99 Hz	1.02 Hz	1.04 Hz
4th Rim Deformation	1.02 Hz	1.03 Hz	1.04 Hz	1.06 Hz

The 1st Y-Direction sway, the torsion, and the 1st X-Direction sway modes are of most concern from an occupant comfort and dynamic load generation perspective and these modes agree very well between the linearized Dynamics models and the corresponding models. The two TMDs are intended to address the Y- and X-Direction sway modes which have modal masses of 9,400 t and 10,500 t, respectively. The torsion mode and the various rim deformation modes also affect passenger comfort to some degree; however, any attempt to control these modes necessitates placement of TMDs in the rim itself.

3. TUNED MASS DAMPER OPTIONS

The Wheel may incorporate tuned mass dampers to reduce the vibration level that capsule occupants will experience and to provide structural load mitigation for worst-case storm conditions. The baseline TMD option places two large TMDs (estimated total mass of 28.5 t each) at the top of each A-Frame that will be designed to control the primary Y- and X-Direction sway modes. The A-Frame-mounted TMDs cannot effectively control the torsion mode of the Wheel, so an alternate arrangement is considered. An alternate approach is to place smaller TMDs (about 1.5 t each) at each capsule. The 36 capsule-mounted dual-mode TMDs may be more effective; however, the limited available space and the higher sway space required for this design render this option more problematic to implement; hence, this study focuses on the evaluation of the A-Frame-mounted TMDs. Several analyses of the alternate capsule-mounted TMDs are performed for comparison.

3.1 A-FRAME-MOUNTED TUNED MASS DAMPER—BASELINE DESIGN

Two tuned mass dampers installed near the apex of each A-Frame is the baseline TMD design. An example of the TMD planned for the Wheel is shown in the left-hand-side of Figure 2. This TMD designed by the manufacturer permits motion in two orthogonal directions. The upper-most active mass (estimated at 24.2 t for the purposes of this study) can move relative to the A-Frame in the X- and Y-Directions, whereas the smaller active mass (estimated at 4.3 t) can only move in Y-direction (the upper mass is constrained to move with the lower mass in the Y-direction). The actual total mass and mass distribution between the upper and lower locations is not known at present, but will be updated with information provided by the TMD design agent as their design matures.

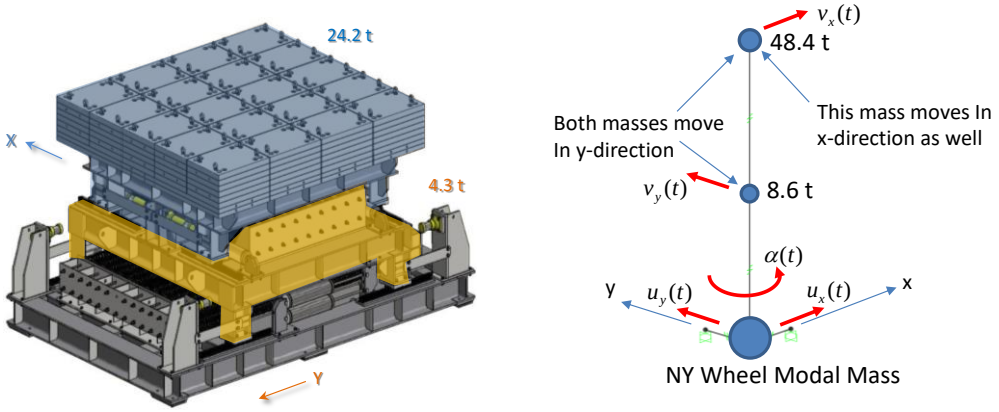

Figure 2 Constrained-Orthogonal-Motion TMD (Left) and Equivalent 4-DOF Model (Right)

The equivalent dynamics model for both TMDs combined is shown in the right-hand-side of Figure 2, where a five-degree-of-freedom (5-DOF) model is defined and used to represent the motion of the A-Frame (3-DOF, 2 for translation and 1 for torsion about the Z-Axis) and the TMD (2-DOF). The A-Frame mass and stiffness are taken from the modal mass of the Y- and X-Direction sway modes and their respective resonance frequencies. The mass of the Wheel superstructure, excluding the A-Frame, is 4,343 t (including the cables) and the mass of the cables is 512 t. These values are used to determine an approximate mass moment of inertia for the wheel about the Z-Axis per

$$I_{ZZ} \approx \left(M_{Wheel} - M_{Cables}\right)\frac{R^2}{2} + M_{Cables}\frac{R^2}{4} = 1.54 \times 10^7 \text{ t} \cdot \text{m}^2, \quad (1)$$

where *R* is radius of the wheel. The mass moment of inertia is used with the torsion mode resonance frequency (0.25 Hz) to determine the torsion spring stiffness for the model. A damping level of 0.5% is assumed for the two sway modes and the torsion mode. The equations of motion for the 5-DOF are given by

$$\begin{bmatrix} M_y+m_y & 0 & 0 & m_y & 0 \\ 0 & M_x+m_x & 0 & 0 & m_x \\ 0 & 0 & I_{zz} & 0 & 0 \\ m_y & 0 & 0 & m_y & 0 \\ 0 & m_x & 0 & 0 & m_x \end{bmatrix} \begin{Bmatrix} \ddot{u}_y \\ \ddot{u}_x \\ \ddot{\alpha} \\ \ddot{v}_y \\ \ddot{v}_x \end{Bmatrix} + \begin{bmatrix} C_y & & & & \\ & C_x & & & \\ & & C_t & & \\ & & & c_y & \\ & & & & c_x \end{bmatrix} \begin{Bmatrix} \dot{u}_y \\ \dot{u}_x \\ \dot{\alpha} \\ \dot{v}_y \\ \dot{v}_x \end{Bmatrix} + \begin{bmatrix} K_y & & & & \\ & K_x & & & \\ & & K_t & & \\ & & & k_y & \\ & & & & k_x \end{bmatrix} \begin{Bmatrix} u_y \\ u_x \\ \alpha \\ v_y \\ v_x \end{Bmatrix} = \begin{Bmatrix} F_y(t) \\ F_x(t) \\ M_z(t) \\ 0 \\ 0 \end{Bmatrix} \quad (2)$$

The simple point-mass model of the TMDs is incorporated into the structural dynamics model of the Wheel as shown in Figure 3. The total TMD mass shown in Figure 2 is equally divided over the two A-Frame locations. The upper point mass can translate relative to the mass below in the X-Direction only—all other degrees of freedom are constrained to match the point mass below. The lower point mass is constrained to move relative to the A-Frame in the Y-Direction only and all other degrees of freedom are constrained to match the A-Frame attachment. The TMD mass, spring stiffness, and viscous damping values in the 5-DOF model are simply halved when used with this dual-TMD model.

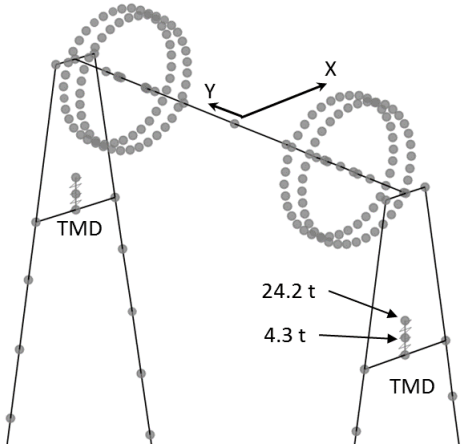

Figure 3 Point-Mass TMDs in the Linearized Structural Dynamics Model

3.2 CAPSULE-MOUNTED TUNED MASS DAMPERS—ALTERNATE DESIGN

The baseline TMDs, located in the A-Frame, do not control the torsion mode of the Wheel. An alternative TMD configuration is considered that can be tailored to address both the torsion and the Y-Direction sway modes. A general-purpose low-order-degree-of-freedom model of the Wheel is developed to explore alternative TMD configurations. The 6-DOF model is shown in Figure 4. The thick bar represents the Wheel structure that is assumed to translate and rotate to emulate the combined Y-Direction sway and torsion modes. The additional degrees of freedom describe the motion of the TMD masses placed a distance *R* from the center of the Wheel. The baseline TMD is obtained by setting $R = 0$, $m_2 = 0$, and $m_1 = 28.5$ mt. The additional mass, m_2, attached to the TMD mass, m_1, may be thought of as a TMD on a TMD and allows the 2-DOF TMD to be tuned to control two closely-spaced modes of a structure (*e.g.*, the torsion and sway modes) instead of just one; *i.e.*, a "dual-mode TMD." The offset applied force, $F(t)$, causes sway and torsion motion. The equations of motion for the 6-DOF model are provided

in Equation (3). SciLab is used to solve this coupled set of 2nd order ordinary differential equations for a given force time history.

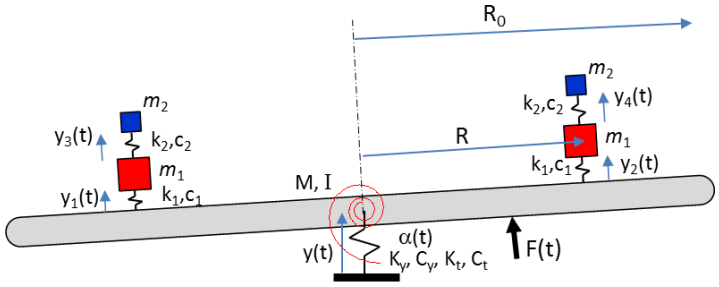

Figure 4 6-DOF Model of the Observation Wheel and TMDs

$$\begin{bmatrix} (M+2m_1+2m_2) & 0 & (m_1+m_2) & (m_1+m_2) & m_2 & m_2 \\ 0 & (I+2m_1R^2+2m_2R^2) & -(m_1+m_2)R & (m_1+m_2)R & -m_2R & m_2R \\ (m_1+m_2) & -(m_1+m_2)R & (m_1+m_2) & 0 & m_2 & 0 \\ (m_1+m_2) & (m_1+m_2)R & 0 & (m_1+m_2) & 0 & m_2 \\ m_2 & -m_2R & m_2 & 0 & m_2 & 0 \\ m_2 & m_2R & 0 & m_2 & 0 & m_2 \end{bmatrix} \begin{Bmatrix} \ddot{y} \\ \ddot{\alpha} \\ \ddot{y}_1 \\ \ddot{y}_2 \\ \ddot{y}_3 \\ \ddot{y}_4 \end{Bmatrix} + \begin{bmatrix} C_y & & & & & \\ & C_t & & & & \\ & & c_1 & & & \\ & & & c_1 & & \\ & & & & c_2 & \\ & & & & & c_2 \end{bmatrix} \begin{Bmatrix} \dot{y} \\ \dot{\alpha} \\ \dot{y}_1 \\ \dot{y}_2 \\ \dot{y}_3 \\ \dot{y}_4 \end{Bmatrix} + \begin{bmatrix} K_y & & & & & \\ & K_t & & & & \\ & & k_1 & & & \\ & & & k_1 & & \\ & & & & k_2 & \\ & & & & & k_2 \end{bmatrix} \begin{Bmatrix} y \\ \alpha \\ y_1 \\ y_2 \\ y_3 \\ y_4 \end{Bmatrix} = \begin{Bmatrix} F \\ F \cdot 0.35R \\ 0 \\ 0 \\ 0 \\ 0 \end{Bmatrix} \quad (3)$$

The dual-Mode TMD assumes the TMD mass is "spread" around the perimeter of the wheel. Hence, the total assumed TMD mass of 57 mt can be reconfigured as 36 smaller TMDs with a mass of 1.58 mt each. The effectiveness of the rim-mounted TMDs to resist the torsion mode is affected by the moment arm of the TMD mass relative to axis of torsional rotation. The effective radial distance for half of the total TMD mass is determined from

$$R_{Eff} = \frac{1}{M_{TMD}} \int_{-\pi}^{\pi} \left(\frac{M_{TMD}}{2\pi R_0} \right) R_0^2 \cos(\phi) d\phi = \frac{2}{\pi} R_0 = 0.637 R_0 \quad (4)$$

In other words, the effect of 36 rim-mounted TMDs with the same total mass as the two TMDs planned for the A-Frame is properly accounted for by placing two 28.5-mt TMDs (m_1+m_2) at R = 0.637R_0 in the 6-DOF model.

The frequency response characteristics of the 6-DOF Wheel model is determined from the ratio of the response at the rim to the excitation in the frequency domain. A half-sine pulse with a duration of 0.1 sec and an amplitude of 1000 kN is applied to the model as shown in Figure 4. The response is the acceleration at R_0. The frequency response function for no TMDs (m_1 = m_2 = 0) is plotted in the right-hand-side of Figure 5. The two peaks in the plot correspond to the torsion and sway modes at 0.25 Hz and 0.28 Hz (assumed damping level is 0.5% for both modes). The amplitude of the response at both modes is set to be roughly the same for this model.

The objective of any vibration mitigation effort is to reduce the level of vibration at the rim. One metric describing the vibration is the maximum amplitude of the frequency response function. This level is the steady state response amplitude for harmonic excitation applied at the frequency where the peak occurs. Another metric is related to the RMS level, which is proportional to the square root of the area under the frequency response curve[1] within a representative frequency band. For the purposes of this comparison, the response from 1/6 octave below the torsion mode frequency (0.22 Hz) to 1/6 octave above the sway mode frequency (0.31 Hz) is considered for the

[1] The magnitude of the frequency response curve is squared when calculating the RMS metric.

RMS metric. A point is plotted in the left-hand-side graph in Figure 5 corresponding to the peak magnitude and RMS level for the no-TMD configuration.

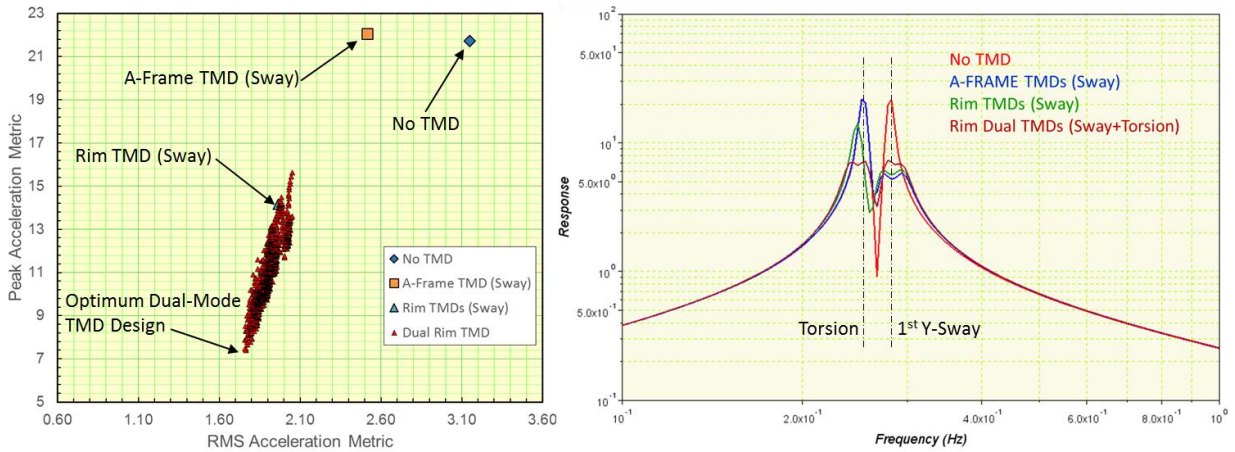

Figure 5 Comparison of Wheel Response for Different TMD Concepts (6-DOF Model)

The effect of two 28.5-mt TMDs located in the A-Frame and tuned to address only the sway mode is computed following the same methodology and 6-DOF model (R = 0, m_2 = 0, m_1 = 28.5 mt). This TMD has no effect on the torsion mode, so the peak response at 0.25 Hz is not reduced with this TMD. There is, however, a significant reduction in the peak at 0.28 Hz (the sway mode). A point corresponding to the peak magnitude and the RMS level is plotted in Figure 5. The peak magnitude is not reduced, because the torsion mode is unaffected. The reduction in the sway mode peak does appear as a reduction in the RMS level.

One option is to replace the two 28.5-mt TMDs with 36 TMDs with the same total mass. These capsule-mounted TMDs are first assumed to be tuned to address the sway mode. The 6-DOF model is updated with $R = 0.637R_0$, m_2 = 0, and m_1 = 28.5 mt, and the resulting frequency response curve is plotted in the right-hand-side of Figure 5. The point corresponding to the reduction in the peak magnitude and RMS level is plotted in the graph in the left-hand-side of the figure. Interestingly, there is some "leakage" benefit of the response reduction at 0.28 Hz at the torsion mode which reduces the peak magnitude. This effect, more than the direct benefit at the sway mode frequency is also responsible for the RMS level reduction.

A traditional TMD is designed to enhance the effective damping in a single mode of the host structure. TMDs are tuned to address one structural mode and have very little effect on the frequency response of the structure at frequencies just below or above the TMD tuning frequency. The challenge here is to control two closely-spaced modes without having to add another TMD and the associated mass (*i.e.*, effectively doubling the added mass and cost). A single-mode TMD can be enhanced to dampen two closely-spaced modes by essentially adding a TMD to the TMD. This is the spring, damper, mass system shown in the 6-DOF model (k_2, c_2, and m_2) in Figure 4. The multiple closely-spaced modes that result when this form of TMD is introduced complicate the tuning process. Various combinations of mass ratio [$r = m_2/(m_1+m_2)$], tuning frequencies f_1 and f_2, and damping level are evaluated. The combination of those parameters that produce a peak acceleration and RMS level closest to the lower left corner of the left-hand-side plot in Figure 5 is the optimum dual-mode TMD design (r = 0.015, f_1 = 0.267 Hz, f_2 = 0.253 Hz, and ξ = 4% of critical). The frequency response curve obtained with the optimum parameters is plotted in the right-hand-side of the figure. The tuning effectiveness of the proposed dual-mode TMD is evident in the frequency response curve by the nearly flat response at both the torsion and the sway modes.

A design concept for the capsule-mounted dual-mode TMD is shown in Figure 6. The three mass elements, m_A, m_B, and m_C all slide in the Y-Direction (normal to the Wheel and parallel to the capsule axis). The very small mass, m_C (0.024 mt), moves independently in the Y-Direction and plays the role of the TMD on the TMD, which allows the TMD to be tuned to the Y-Direction sway mode and the torsion mode. Hence, a very small piggy-back mass is all that is required effectively control two, instead of just one, mode. The two masses, m_B and m_C, also move in the X-Direction to provide damping for the X-Direction sway mode. The size of the TMD shown in the figure is drawn to scale, but the actual shape and location within the capsule footprint can be altered to fit within the available space if, in fact, there is space available.

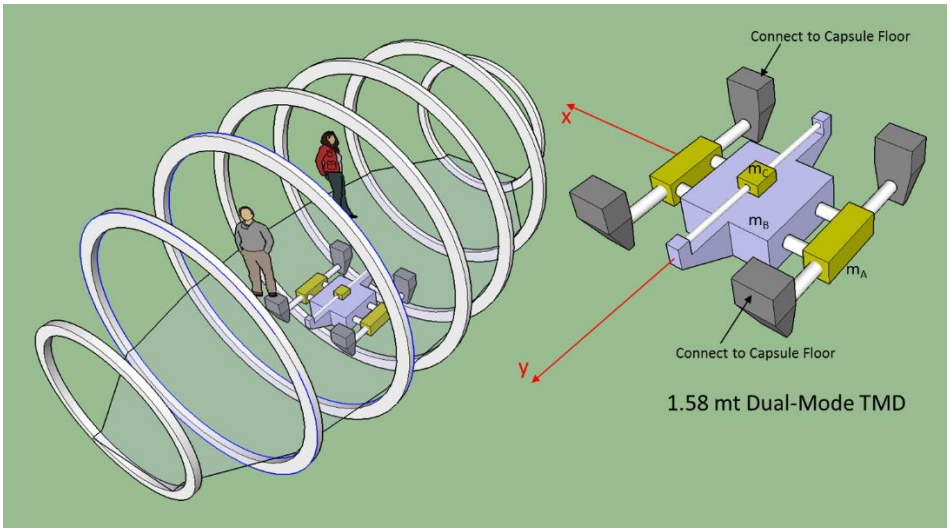

Figure 6 Illustration of Capsule-Mounted 3-DOF Dual-Mode TMD Concept

4. WIND FIELD DATA

Wind field force time histories are provided for use in this investigation. All wind force time histories represent wind directions normal to the plane of the wheel. Two different 3-second gust wind speeds at 10 m above grade are used: 20 m/s for an operating condition and 43.8 m/s for the strength design (storm) condition. Wind forces are provided for an over-land approach (220° rel North) and an over-water approach (40° rel North). A summary of the wind cases is provided in Table 2.

Table 2 Summary of Wind Force Conditions

Case	Direction	*V*, 3-sec Gust at 10 m
1	40° rel North	20 m/sec
2	220° rel North	20 m/sec
3	40° rel North	43.8 m/sec
4	220° rel North	43.8 m/sec

There are ten (10) 1-hour-long time series with a time increment of 0.05 seconds within each of the four cases. The ten simulations for each combination of wind speed and direction are nominally identical except for run-to-run random variability. Separate wind force time history files are provided for each of the 36 capsule locations for the capsule+rim force (F_x, F_y, F_z) and for the cable force (F_x, F_y, M_z). An additional file is provided for the total cable force at the spindle. Files are also provided for the six base reaction forces and moments produced by the A-Frame. In total, 225 files are provided for each of the 40 simulations (9000 files).

It is neither necessary nor practical to perform complete structural dynamics analyses with the Dynamics model for the complete wind force time history library, so a rational approach for identifying the critical wind force time histories and analyses is developed (see Section 5.2). It is also necessary to investigate the response of the Wheel to wind directions other than normal to the plane of the Wheel. Drag force data are used to develop approximate oblique incidence wind force time history files to facilitate these analyses.

4.1 WIND FORCE DATA PROCESSING

The wind forces acting in the X- and Z-Directions are incidental, given that the wind direction is aligned with the model Y-Axis. All of the forces acting at the 36 capsule locations, spindle, and A-Frame were combined into a total force in the Y-Direction for comparison purposes. The mean total wind force (base shear) in the Y-Direction is about 35% higher for the 40° wind direction (over-water approach); hence, from a static or quasi-static analysis perspective, the wind force time history files for the over-land approach (Cases 2 and 4 in Table 2) may be ignored.

Power spectra for the time-varying component of the wind force are plotted in Figure 7 for the total force in the Y-Direction and a representative rim/capsule force (at the top of the Wheel), all from Simulation 5[2]. The colored lines in the plot correspond to the 40° wind direction and the thin black lines immediately below each colored line correspond to the 220° wind direction. The power spectra show the variability in wind force as a

[2] The statistical variation in Simulation N is the same for each Case (wind speed and direction), but is not correlated with Simulation M, where N ≠ M.

function of frequency. As might be expected, the variability is greatest for the higher wind speed and lowest for the single-point contribution at a capsule. The variability in the wind force is the vibration-inducing component of the wind force time histories and its magnitude is correlated with the mean wind force. Therefore, for each case (wind speed and direction), there is less variability in the 220° direction than in the 40° direction because the power spectral density (PSD) is less for the 220° direction than for the 40° direction across the frequency range. This comparison applies for the other simulations as well, leading to the general conclusion that the 40° wind direction controls for static and dynamic analyses.

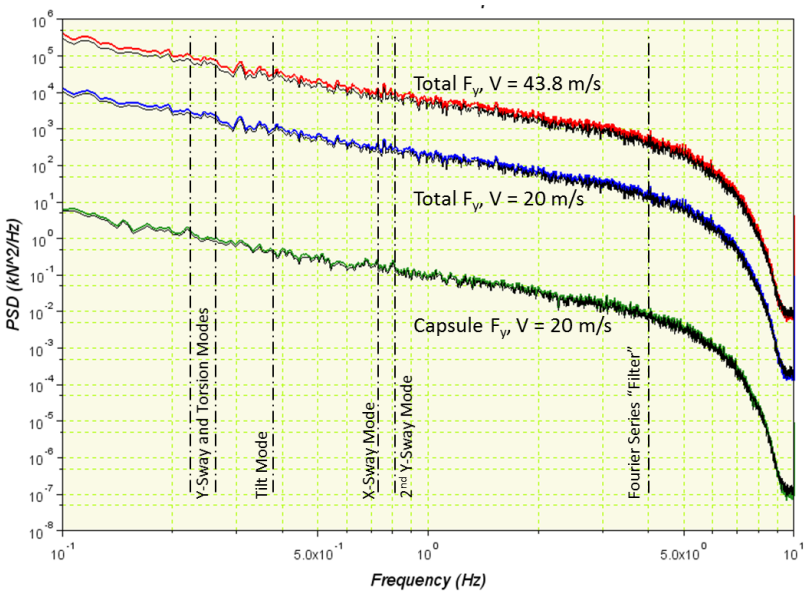

Figure 7 Simulated Wind Force Power Spectra

The magnitude of the power spectra decrease rapidly with frequency, which indicates the lower-frequency modes of the Wheel (*e.g.*, the Y-Direction sway mode at 0.23 Hz or 0.28 Hz) are much more susceptible to wind-induced excitation than the higher-frequency modes (*e.g.*, the X-Direction sway mode at 0.74 Hz). Finally, there are no peaks in the wind force power spectra that would indicate the presence of critical excitation frequencies that could excite a structural resonance where one might expect magnified response.

The first 12 minutes of a simulated force time history is shown in Figure 8—the linear ramp is included by the wind tunnel consultant as a standard feature to reduce the start-up transient in dynamics analyses. The original time series are modified before use in the structural dynamics response analyses performed for this investigation. First, the initial linear ramp is deleted and the mean force (post ramp) is subtracted from each of the time series files. The mean (static) forces are saved as a corresponding set of forces that may be used in a nonlinear static analysis with the original nonlinear model. The modal analysis results shown in the "Pre-Loaded State" column of Table 1 are computed based on the pre-loaded model that includes the static wind forces extracted from these simulations.

The modified wind force time history files contain only the zero-mean dynamic component of the wind force. The combined net force full-length wind force time histories are analyzed using the 5-DOF dynamics model of the Wheel structure to identify the worst-case period as discussed in Section 5.1. Smaller subsets of the histories, about 3 to 4 minutes in duration, are extracted for analysis with the Dynamics model of the Wheel. These isolated, shorter-duration, force time histories are further processed to improve numerical solution accuracy.

A 10-second-long half-period cosine window is applied to the beginning and the end of the extracted time series to ensure that the initial and final force and slope (force/second) are zero. The windowed time series is then replaced with a Fourier series representation, where the number of terms used in the Fourier series is selected to provide excitation up to 4 Hz[3]. The Fourier series representation provides an effective means of filtering the original force time histories to prevent higher-frequency structural modes from contributing unrealistically (via numerical instability) to the final response and allows the force time histories to be sampled at a finer time increment, if desired, that further guards against numerical instabilities arising from the high-frequency modes. A comparison of a 200-second-long time history and its Fourier series are shown in Figure 9 with an inset zoomed-in view showing the agreement between the original time series and the Fourier series representation.

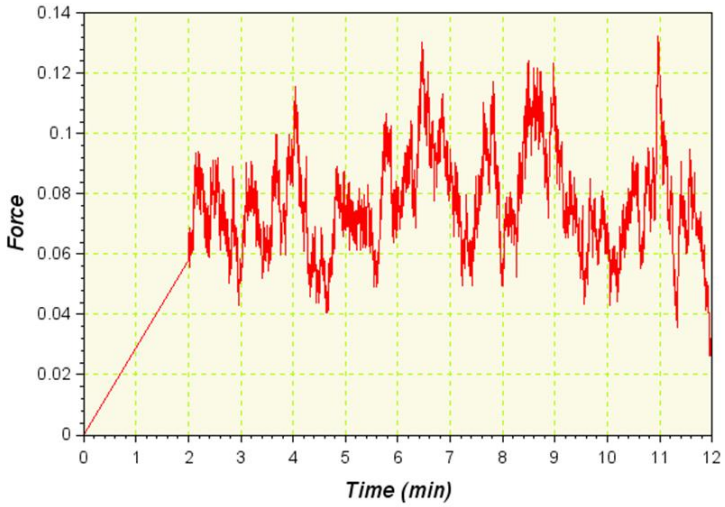

Figure 8 Example of Raw Wind Force (in kips) Time History File

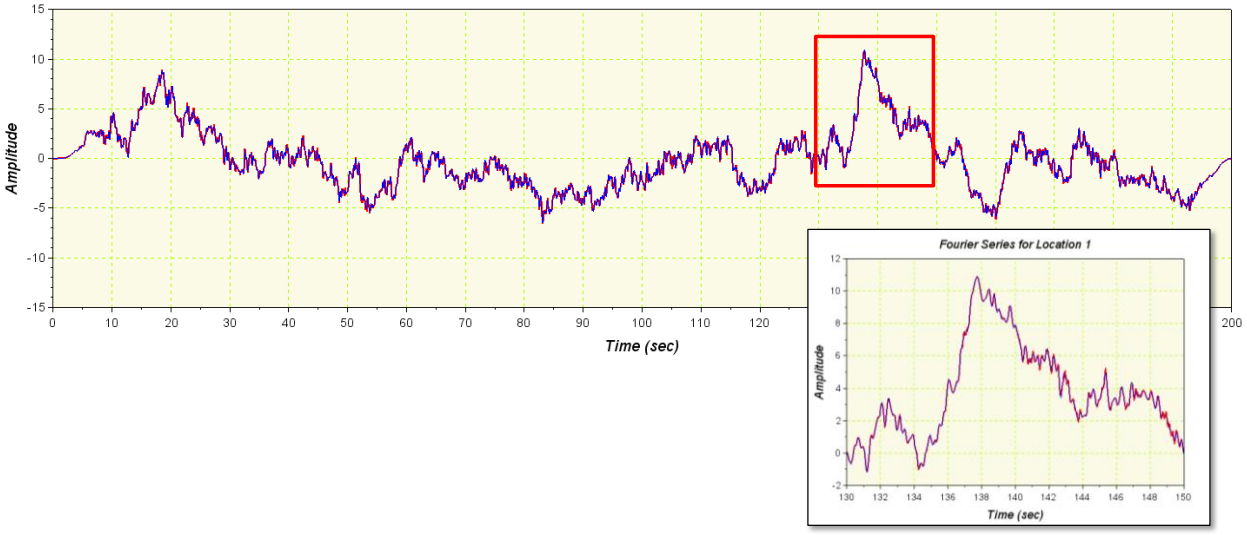

Figure 9 Fourier Series Representation of the Force Time History

[3] This is the Fourier Series "Filter" line shown in Figure 7

4.2 OBLIQUE WIND INCIDENCE

The TMDs are intended to control the motion of the Wheel in two directions: normal to the plane of the Wheel and parallel with the plane of the Wheel; however, the wind force time history files are for wind directions normal to the plane of the Wheel only. These forces are provided for three separate elements: the A-Frame, the Cables, and the Capsule/Rim. The final drag report contains drag coefficients for alternate wind directions and different azimuthal locations around the rim for the Capsule/Rim component and this information is used here to develop wind force time histories for off-normal wind incidence angles, particularly for the 90° case (*i.e.*, wind parallel to the plane of the Wheel). Intermediate angles of wind incidence are assessed to verify that that the controlling cases for the Wheel's response and TMD design occur for the normal and parallel wind directions.

The normal-incidence forces applied to the A-Frame and Cables are simply scaled by the sine and cosine of the wind direction angle measured relative to the normal ($\theta = 0°$ is normal to the wheel as shown in Figure 10). The cable forces are additionally adjusted in the X-Direction to account for their inclination toward the wind vector. The drag coefficients for the Capsule/Rim for a 90-degree variation in wind direction and azimuthal location around the rim, ϕ, are provided in the Drag Force Report, and are shown in Figure 11. The Y-Direction Capsule/Rim forces are obtained by simply scaling the normal-incidence forces by $\cos(\theta)$ as this appears to be in reasonable agreement with the data (the solid line shown in the left-hand-side of Figure 11). A more complicated relationship exists for the X-Direction component where the cross-wind wind vector varies between normal to the rim ($\phi = 0°$) and parallel to the rim ($\phi = 90°$). The drag coefficient for the X-Direction component is obtained from the data shown in the right-hand-side of Figure 11 using linear interpolation with respect to θ and ϕ.

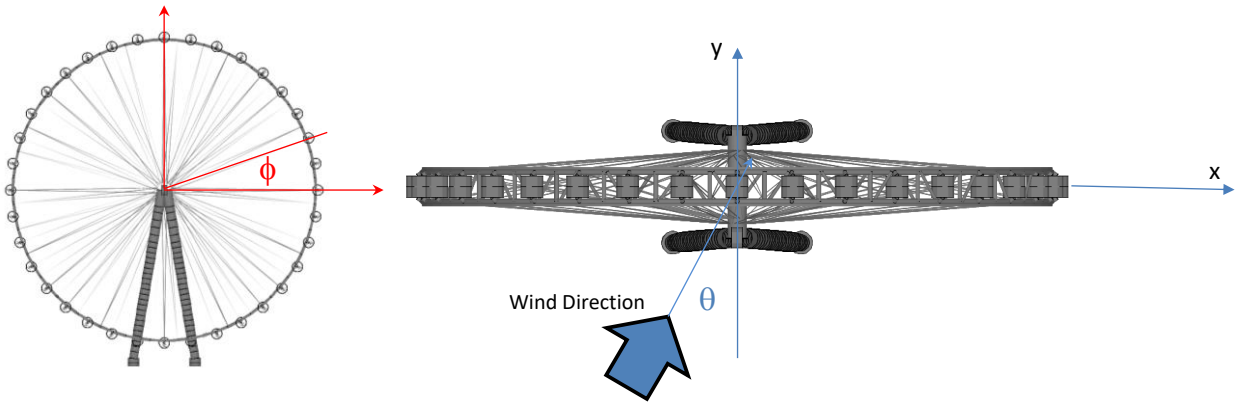

Figure 10 Oblique Wind Direction Geometry

The total base shear and overturning moment are computed for the 10 unique simulations that comprise Case 1 (wind direction = 40° rel North at 20 m/s) and then adjusted for wind incidence angles between 0° (parallel to the Y-Axis) and 90° (parallel to the X-Axis) and plotted in Figure 12. The net wind force and moment do not vary significantly over the 10 simulations so there is very little difference between the 10 nominally-identical curves. The corresponding forces for the 43.8 m/s wind case (Case 3) may be obtained by simply scaling these results by the square of the wind velocity ratio $[(43.8/20)^2 = 4.8]$[4].

[4] The ratio of the forces is actually closer to 4.4.

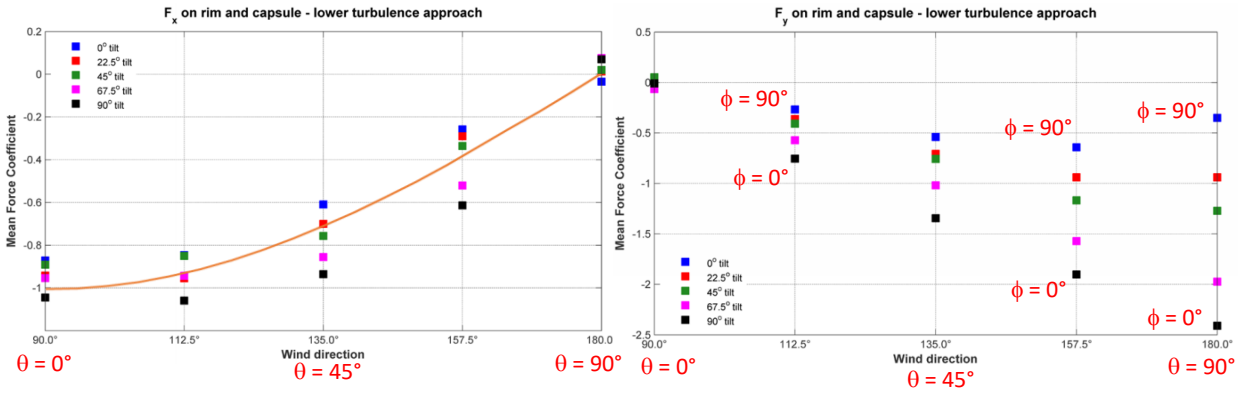

Figure 11 Drag Coefficients from the Final Drag Forces Report

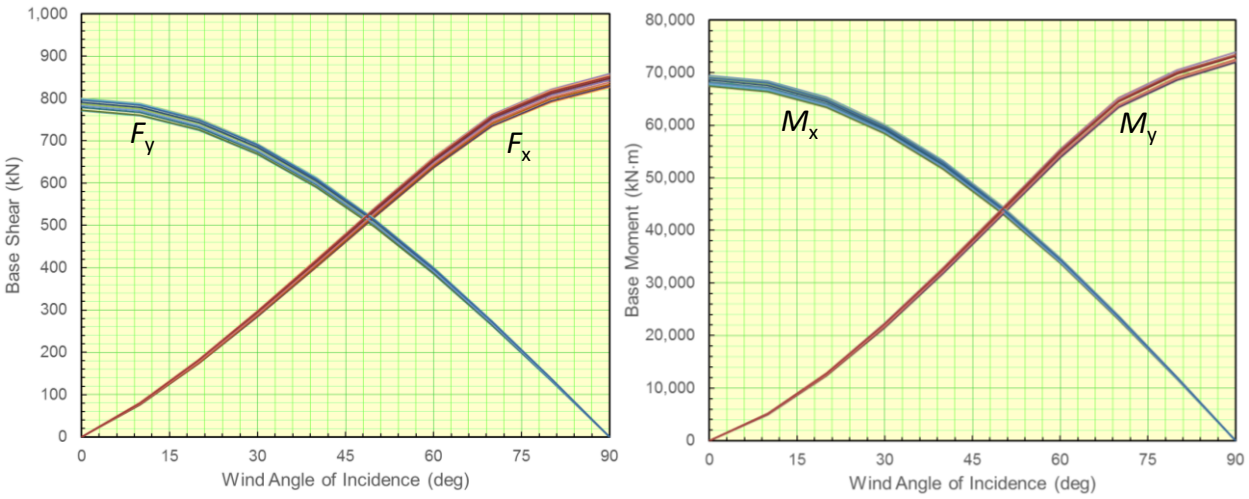

Figure 12 Variation in Base Shear (Left) and Moment (Right) with Oblique-Incident Wind Angle

The dynamic wind forces for wind incidence angles other than 0° are also obtained using this procedure. These forces are then used in the time history response analyses to assess the dynamic response of the Wheel in combined-direction motion for $\theta° > 0$ and for the maximum response in the X-Direction ($\theta \approx 90°$). This study focuses on the worst-case wind direction angles of 0° and 90°.

5. STRUCTURAL DYNAMICS RESPONSE

A comprehensive series of the Wheel dynamics simulations is performed to identify worst-case design forces for the structural members and to define the peak acceleration around the rim as a prelude to evaluating occupant comfort. The applied forces used to define the maximum design forces are taken from the 43.8-m/s 3-sec gust wind speed (storm condition), while the peak rim acceleration assessment is based on the 20-m/s 3-sec gust wind speed (operating condition). The acceleration response is assessed with and without the TMDs to gauge their effectiveness. Analyses are performed for a Y-Direction sway mode frequency of 0.23 Hz and 0.28 Hz as observed in Table 1 for the initial state and preloaded state modal analyses.

5.1 DYNAMICS SIMULATION ACCURACY

The SAP2000 numerical algorithms used to solve the equations of motion are well-established; however, it is the analyst's responsibility to select an appropriate time step to ensure an accurate solution. A large time step can lead to numerical instability that is easily identifiable as a bad solution. It may be possible to select a stable time step, but still obtain an inaccurate solution. Some numerical integration algorithms introduce artificial damping in a solution that would lead to an under-prediction of the Wheel's motion and an overly optimistic assessment of passenger comfort and dynamic-induced structural loads.

A free vibration analysis is performed to assess the damping in the response. A proportional damping model is assumed in the solution where the Y- and X-Direction sway modes (0.23 Hz and 0.74 Hz, respectively) are assigned critical damping values of 0.5%. A force is gradually applied from 0 kN to 1,000 kN over a 5-sec period in the Y-Direction along the axis of the spindle and then removed. A half-cosine ramp is used in the damping assessment simulation so that the applied force is gradually applied and released. This approach minimizes the participation of higher-frequency modes that complicate the damping assessment.

Once the force is released, the structure "springs" back to its undeflected shape after numerous oscillations back and forth around the final equilibrium position. The acceleration should follow the theoretical solution for a single-degree-of-freedom system undergoing free vibration given by

$$\ddot{u}_y = a_{\max} \sin\left(2\pi f_n \sqrt{1-\xi^2}\, t\right) e^{-2\pi f_n \xi t}, \tag{5}$$

where $a_{\max}$ is the maximum acceleration that occurs after the force is released, $t = 0$ is the time measured from the peak acceleration, f_n is the resonance frequency in Hz, and ξ is the critical damping factor for the mode.

The acceleration response at the center of the spindle is plotted in Figure 13 along with the theoretical free vibration response from Equation (5). The theoretical solution is shifted in time and adjusted in amplitude to achieve the best-possible agreement between the theoretical solution and the SAP2000 solution ($\Delta t = 0.0025$ sec). The agreement is excellent after the 5-sec cosine ramp, which indicates the algorithm and time step used for analysis are providing an accurate solution as far as damping is concerned.

The solution presented in Figure 13 does not provide insight into the amplitude accuracy because the $a_{\max}$ term in the theoretical response is adjusted to match the SAP2000 solution. Also, care was taken to avoid unintentional excitation of higher frequency modes that are a primary source of numerical error. The solution accuracy is assessed using the free vibration response, except that a linear ramp is used. The linear ramp causes additional structural modes to be excited because of the rapid application and release of the force. There is no theoretical solution to compare, so a numerical solution obtained with a smaller time step ($\Delta t = 0.001$ sec) is used as "truth" in this case. Both computed acceleration responses are plotted in Figure 14. There is no difference in the

two solutions. Numerical solutions obtained with Δt = 0.0025 sec are considered to be accurate for the purposes of this analysis effort. It is worth noting that a numerical solution was also obtained with Δt = 0.005 sec and that solution proved to be unstable. All of the numerical solutions obtained in this study are obtained with Δt = 0.0025 sec.

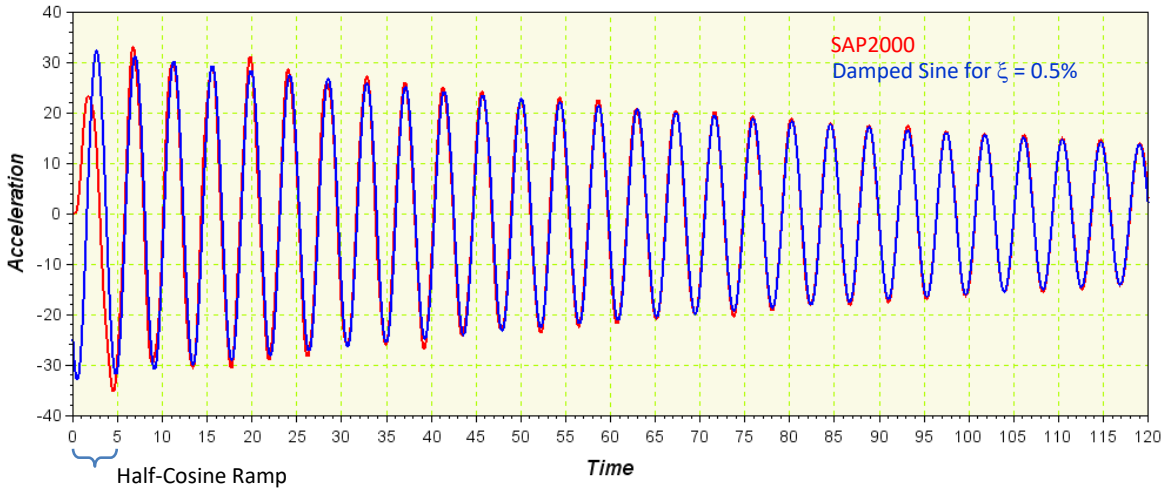

Figure 13 Numerical Integration Damping Accuracy

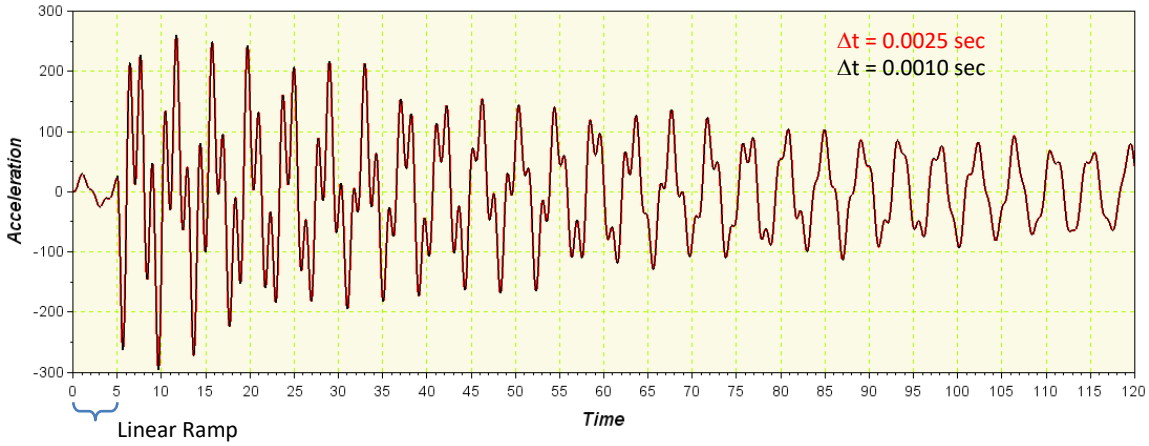

Figure 14 Numerical Integration Amplitude Accuracy

5.2 IDENTIFYING CONDITIONS FOR MAXIMUM RESPONSE

A practical difficulty arises in that the computer analysis time, the size of the output files created, and the consequent difficulty in working with those files precludes performing structural dynamics simulations with the wind force time history files as-is to identify the worst-case structural response. Nor can the maximum force in force time history be used to identify the worst-case response because the presence of a maximum force does not

imply maximum response for a dynamic system. An alternative approach is adopted to identify portions of the wind force time histories that may be responsible for the peak structural responses of interest.

The net force time history (total combined force from the A-Frame, Rim and Capsules, and Cables) in the Y-Direction, the X-Direction (when oblique wind directions are considered), and the net moment about the Z-Axis are applied to the Wheel mass of the 5-DOF dynamics model shown in the right-hand-side Figure 2. The computer analysis time required to obtain the dynamic response of the 5-DOF is only about 10 minutes for an hour-long wind force time history. This model provides the translational accelerations in the X- and Y-Directions ($\ddot{X}$ and $\ddot{Y}$, respectively) and the angular acceleration about the Z-Axis ($\ddot{\alpha}$). The maximum acceleration at the passenger capsules is estimated from the response time histories per

$$a_{Capsule}(t) = \ddot{u}_y(t) + R\ddot{\alpha}(t) \tag{6}$$

The maximum predicted capsule acceleration, TMD displacement, and TMD-to-A-Frame force obtained from the 5-DOF model are summarized in Table 3 for the Y-Direction sway resonance set to 0.28 Hz (per the linearized Dynamics rev1 model) for the 40° wind direction (over-water approach) case. A similar table is provided in Table 8 in Section 7.1 for the 0.23-Hz sway mode. These results are not as accurate as those provided by the full dynamics model because they do not include the contributions of other modes (*e.g.*, rim deformation, tilt, and the 2nd Y-Direction sway) or the accurate distribution of wind forces around the Wheel; however, these do identify the portion of the wind force time history where the maximum response is expected. The much smaller section of the wind force time history can then be extracted and analyzed using the full dynamics model.

Table 3 Summary of 5-DOF Simulation Peak Results (f_Y = 0.28 Hz)

Sim	Wind Force Case: 20 m/s @ 40° rel. North (Case 1)					
	Accel	Time	$Disp_{TMD}$	Time	$Force_{TMD}$	Time
1	16.1 mg	40.4 min	252 mm	25 min	21.2 kN	25 min
2	16.0 mg	52.9 min	197 mm	2.6 min	16.5 kN	2.6 min
3	16.5 mg	9.6 min	180 mm	6.2 min	15.1 kN	6.2 min
4	15.2 mg	8.8 min	238 mm	15.2 min	20.0 kN	15.2 min
5	19.5 mg	8.6 min	174 mm	11.1 min	15.4 kN	11.1 min
6	17.1 mg	18.8 min	177 mm	42.1 min	15.6 kN	42.1 min
7	18.0 mg	40.3 min	205 mm	33.6 min	18.1 kN	33.6 min
8	13.7 mg	5.9 min	214 mm	6.0 min	18.9 kN	6.0 min
9	16.3 mg	18.4 min	255 mm	53 min	22.5 kN	53 min
10	17.3 mg	32.1 min	182 mm	53.9 min	16.0 kN	53.9 min

The capsule acceleration and TMD displacement relative to the A-Frame from the nearly hour-long simulated wind force time history that produced the maximum capsule acceleration (Simulation 5) are shown in Figure 15. The maximum capsule acceleration (with the TMD) is 19.5 mg, which occurs at 8.64 minutes into the response. This same force time history produces a maximum capsule acceleration of 26 mg without the TMD. The maximum TMD motion does not occur at this same time or even in this same response. The maximum TMD

displacement for Simulation 5 is 174 mm; however another simulation, Simulation 9, produced a TMD displacement of 255 mm. Higher TMD motion is an indication that the wind force time history contains a greater proportion of correlated excitation near the frequency that the TMD is tuned to mitigate and is therefore a good indicator of where maximum response is expected with no TMDs.

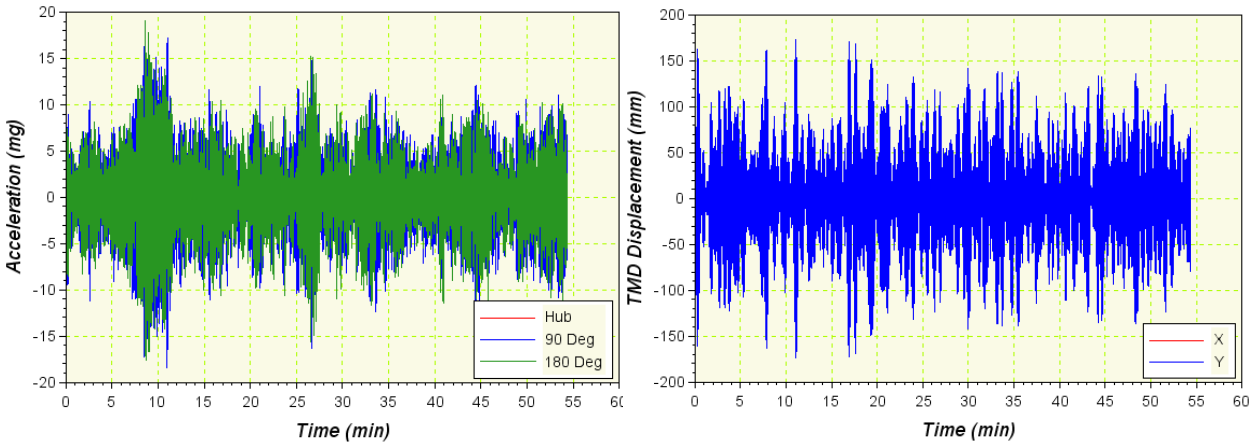

Figure 15 Capsule Acceleration (Left) and TMD Displacement (Right) from 5-DOF Solution

5.3 DYNAMIC RESPONSE WITHOUT TUNED MASS DAMPERS

The response of the Wheel structure without the benefit of the TMDs is considered in this section. The X-Direction responses for several worst-case conditions for the 20-m/s wind speed are plotted in Figure 16 as a function of position around the rim. The response is fairly consistent, indicating the rim translates without deformation (as expected for vibration in this direction).

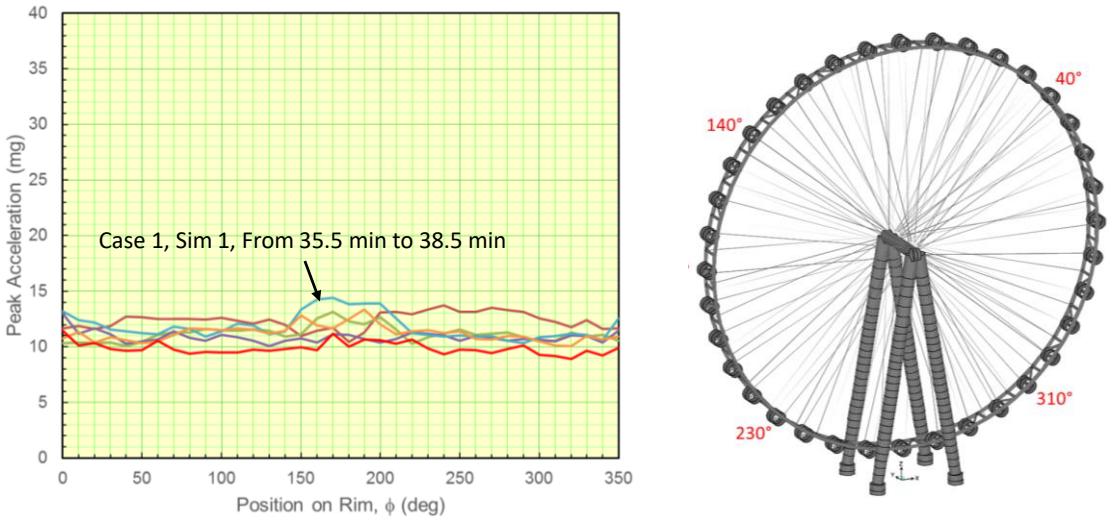

Figure 16 X-Direction Acceleration Response Time Histories

The maximum acceleration around the rim for the 20-m/s wind normal to the plane of the Wheel are plotted in Figure 17 for the 0.23-Hz sway mode frequency (left-hand side) and the 0.28-Hz sway mode frequency (right-hand side). The maximum acceleration is about 35 mg for both cases and occurs near the top of the Wheel where motion associated with tilt mode adds to the sway motion. The minimum acceleration occurs at $\phi = 270°$ for the 0.28-Hz sway mode where the wheel is pushed against the drive mechanism. This additional constraint is not as evident for the smaller motions associated with 0.23-Hz sway mode.

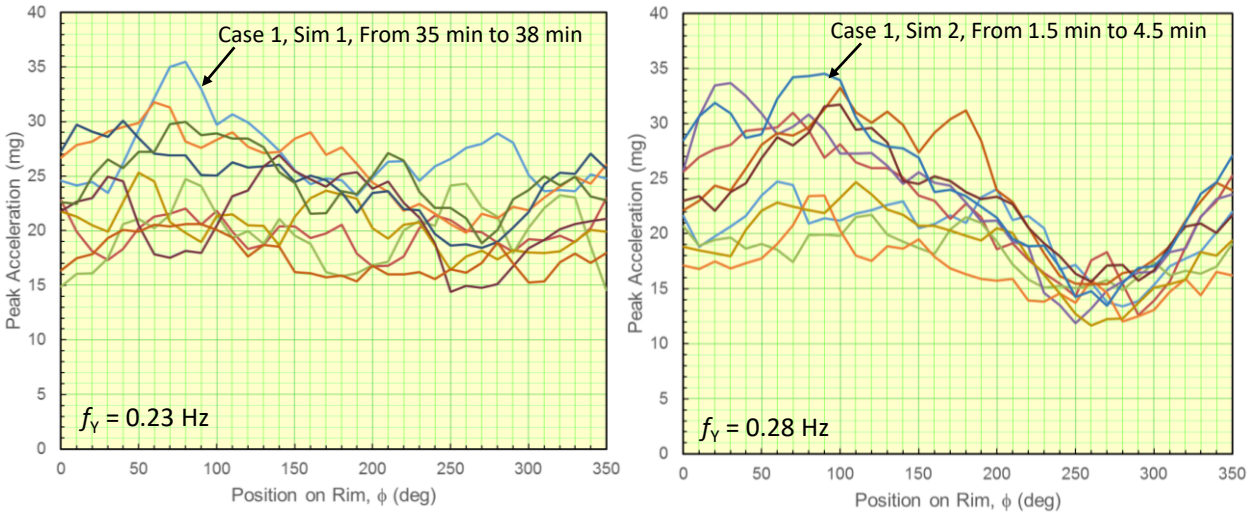

Figure 17 Y-Direction Acceleration Response Time Histories for f_Y = 0.23 Hz (Left) and f_Y = 0.28 Hz (Right)

Frequency-domain analysis of the time history response provides valuable insight into the primary contributors to the motion responsible for the peak accelerations noted in Figure 17. The power spectra from one of the worst-case simulations are plotted in Figure 18 (f_Y = 0.28 Hz) for three different locations on the rim and at midspan on the spindle. Peaks in the power spectra occur at frequencies that identify the structural modes responsible for the vibration.

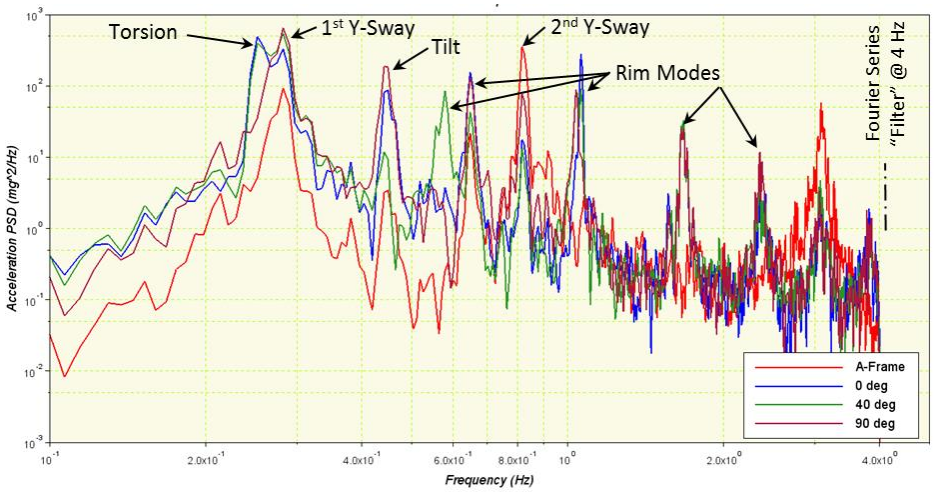

Figure 18 Y-Direction Acceleration Response Power Spectra

The two capsule locations at $\phi = 0°$ and $\phi = 40°$ show a peak response at 0.25 Hz, which corresponds to the torsion mode. The 90°-location and the spindle (A-Frame) do not experience the torsion motion because the axis of rotation for this mode passes through these locations. The highest vibration levels on the rim are associated with the 1st Y-Axis sway mode. The top of the Wheel is more sensitive to the tilt mode than the other locations. Most of the other peaks in the rim power spectra are associated with the various rim deformation modes. There is a relatively high A-Frame response at the 2nd Y-Axis sway mode, but the rim (and passenger capsules) do not experience this motion to the degree that the A-Frame does. The A-Frame also responds to the 2nd flexural mode of the A-Frame legs at about (3.1 Hz), but, once again, the rim is effectively isolated from this motion. There is essentially no response for frequencies greater than 4 Hz because the Fourier series representation of the wind force time histories used in the analysis has no frequency content beyond 4 Hz.

5.4 PASSENGER COMFORT ASSESSMENT: OPERATIONAL WINDS

Passenger comfort is an important consideration in the design of the Wheel. No two people perceive motion the same way or are equally sensitive to motion. Comfort assessment criteria are defined in several ways. One approach defines a limit for the maximum peak acceleration which is typically governed by motion at a critical resonance frequency of the structure. An alternative independent approach employs a limit on the root-mean-square (RMS) acceleration within a frequency range (bandwidth) where people tend to be most sensitive to vibration. This approach is adopted by ISO 2631.

Peak acceleration criteria for tall buildings with resonance frequencies similar to the Wheel generally recognize 40 mg as a peak acceleration level that can cause people discomfort and possibly to lose their balance. The 10-mg level is just perceptible and can be annoying if experienced for a relatively long period of time. The peak acceleration is determined from the root-sum-square (RSS) combination of orthogonal acceleration components and is not filtered based on a “high sensitivity” frequency range (*e.g.*, as per ISO 2631).

The health, comfort, and motion sickness provisions in ISO 2631 are adopted for this project. Vibration levels that satisfy the comfort criterion automatically satisfy the much higher-vibration defined for the health effects criterion. Motion sickness effects are most critical for frequencies below 0.5 Hz, however, this criterion applies in the vertical direction (foot to head). Wind-induced motion in the vertical direction is negligible for the Wheel, so motion sickness is not a concern based on the dominant direction of vibration of the Wheel. The comfort criterion is applicable and ISO 2631 defines a frequency-weighted RMS acceleration level of 32 mg_{RMS} as “Not Uncomfortable.” The frequency-weighting employed by ISO 2631 recognizes that people are more sensitive to motion within a certain frequency range and defines a weighting filter, W_d, to be used for assessing comfort. For vibration that is predominantly sinusoidal in nature (*e.g.*, resulting mostly from a single resonant mode of the structure), the 20-mg peak acceleration limit is more restrictive.

Structural dynamics analyses are performed with SAP2000 to predict the time history response of the Wheel to the wind force time histories provided. These analyses provide the acceleration time histories at any location on the Wheel and power spectra are computed from each of the three orthogonal acceleration time series for that location. The acceleration time histories and corresponding power spectra for the worst-case condition and location on the Wheel are plotted in Figure 19.

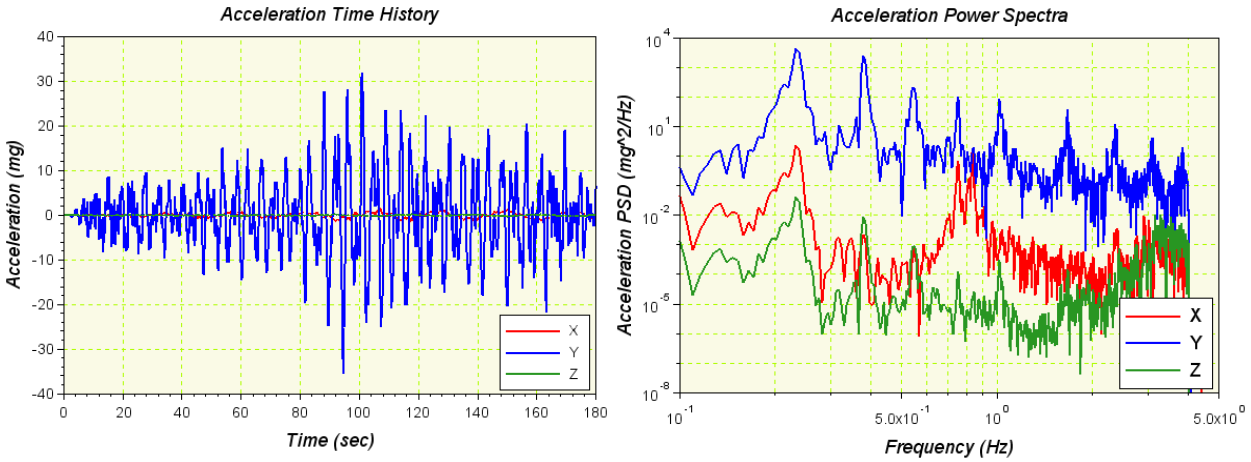

Figure 19 Predicted Acceleration Time Histories (Left) and Power Spectra (Right)

The RMS-weighted acceleration is computed from the power spectra per Equation (7) where $S_d(f)$ is the power spectral density in mg^2/Hz at frequency, f, the subscript, d, refers to the acceleration response direction (x, y, or z), W_{ISO} is the ISO 2631 weighting filter, and f is the frequency bin width associated with the power spectra.

$$a_w = \sqrt{\left(\sum S_x(f)\cdot W_{ISO}^2(f) + \sum S_y(f)\cdot W_{ISO}^2(f) + \sum S_z(f)\cdot W_{ISO}^2(f)\right)\Delta f}\,, \tag{7}$$

The summation is carried out over the full frequency spectrum. The peak and RMS capsule accelerations obtained from the worst-case simulation are plotted in Figure 20 as a function of angular location around the Wheel with and without the TMDs.

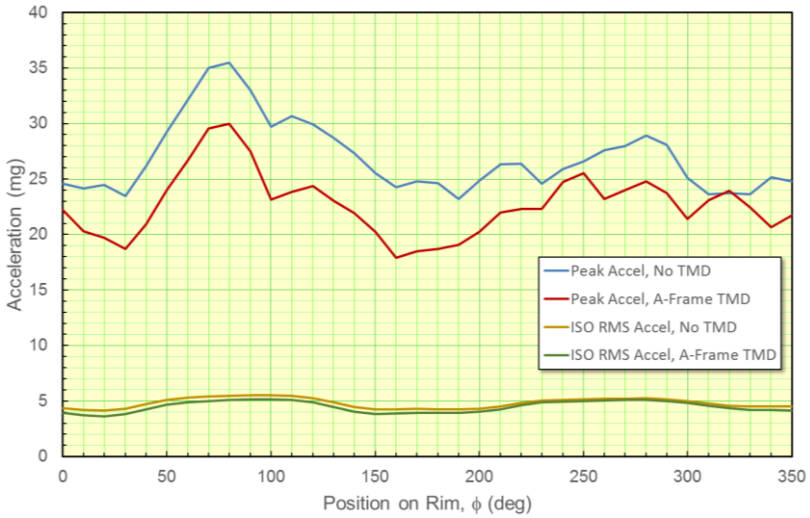

Figure 20 Peak and RMS Accelerations at Passenger Capsules

The peak acceleration levels are about 15% to 20% lower with TMDs. The RMS acceleration is well below the ISO 2631 comfort limit of 32 mg_{RMS} with a crest factor less than 3. The TMDs do not provide any significant mitigation relative to the ISO comfort metric because the TMDs are tuned to the lower sway mode frequency

(0.23 Hz) and therefore provide essentially no mitigation at the higher frequency (1 Hz) where people are most sensitive to acceleration per the ISO 2631 comfort criterion. The peak acceleration occurs at the primary sway mode resonance frequency so the TMDs are much more effective in reducing the peak acceleration levels.

The design basis for the maximum operational wind speed is 20 m/s; however, the operating authority for the Wheel will likely limit public access to the Wheel for wind speeds in excess of 13.4 m/s. The accelerations shown in Figure 20 are computed for a 20-m/s wind speed, but may be scaled by the ratio of the square of the wind velocity; hence, the expected peak acceleration without TMDs drops to about 16 mg (13 mg with the TMDs). These governing RMS accelerations are summarized in Table 4.

Table 4 Summary of RMS Accelerations (No TMDs)

Condition	Acceleration
ISO 2631 Limit	32 mg_{RMS}
V_{Wind} = 20 m/s	5.5 mg_{RMS}
V_{Wind} = 13.4 m/s	2.5 mg_{RMS}

The Wheel satisfies the ISO 2631 comfort criterion for wind speeds in excess of the maximum operational wind speed of 20 m/s. Assessing occupant comfort is more of an art than a science due to physiological variability, influences of gender and age, and mindset (*e.g.*, trying to work or sleep versus sightseeing activity); however, the predicted motions of the Wheel occupant capsules easily satisfy the ISO 2631 comfort criterion.

The TMDs are not required to satisfy the ISO 2631 occupant comfort criterion; however, the TMDs will function in low to moderate winds and will reduce the peak capsule acceleration. The maximum relative displacement of the TMDs in the Y-Direction under operating wind condition is less than ±260 mm and less than ±10 mm in the X-Direction. State-of-the-art wind tunnel test methods, structural dynamics modeling and analysis techniques provide best-possible estimates of the expected Wheel response. Nevertheless, real-world wind forces and structural dynamic response can vary from model predictions and the TMDs will compensate for higher-than-expected real-world motions that some occupants might otherwise find objectionable.

5.5 TUNED MASS DAMPER RESPONSE: STORM WINDS

Passengers will not be allowed access to the Wheel in storm conditions, so the TMDs are not required for occupant comfort in the event of extremely high winds. The TMDs are still effective in providing structural load mitigation for the A-Frame structure under storm wind conditions as their motion helps to dampen the growth of potentially-damaging resonant-like responses that can develop under sustained high winds.

Structural dynamics analyses are performed for worst-case storm-level winds (43.8 m/s) to determine the free sway space required for the active TMD mass, the maximum forces transmitted to the A-Frame supports, and the structural load mitigation that can be expected during the worst-case storm events. The acceleration response at the A-Frame with and without the TMDs and the relative TMD displacement for two worst-case Y-Direction simulations are plotted in Figure 21 and Figure 22. The analysis run numbers may be found in the run matrix provided in Section 7.2. These analyses represent the maximum TMD responses extracted from hours of simulated wind force time histories for a worst-case storm event and therefore have a very low probability of occurrence during the lifetime of the Wheel.

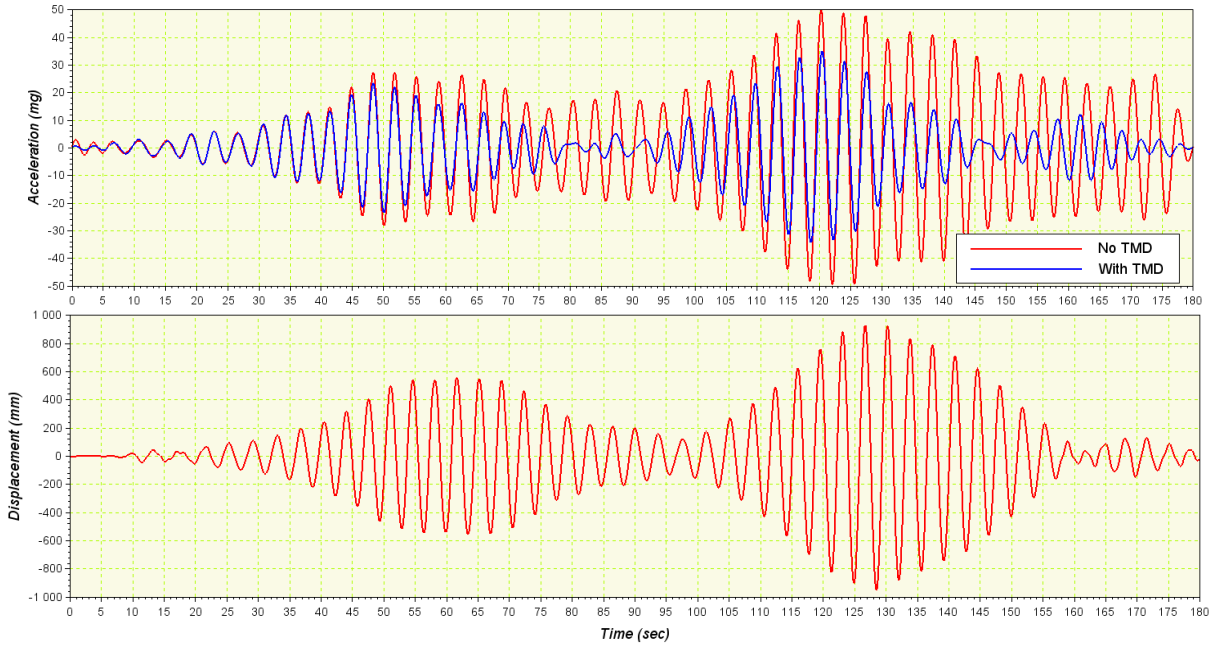

Figure 21 A-Frame Acceleration (Top) and Relative TMD Displacement (Bottom), Runs 65 and 66

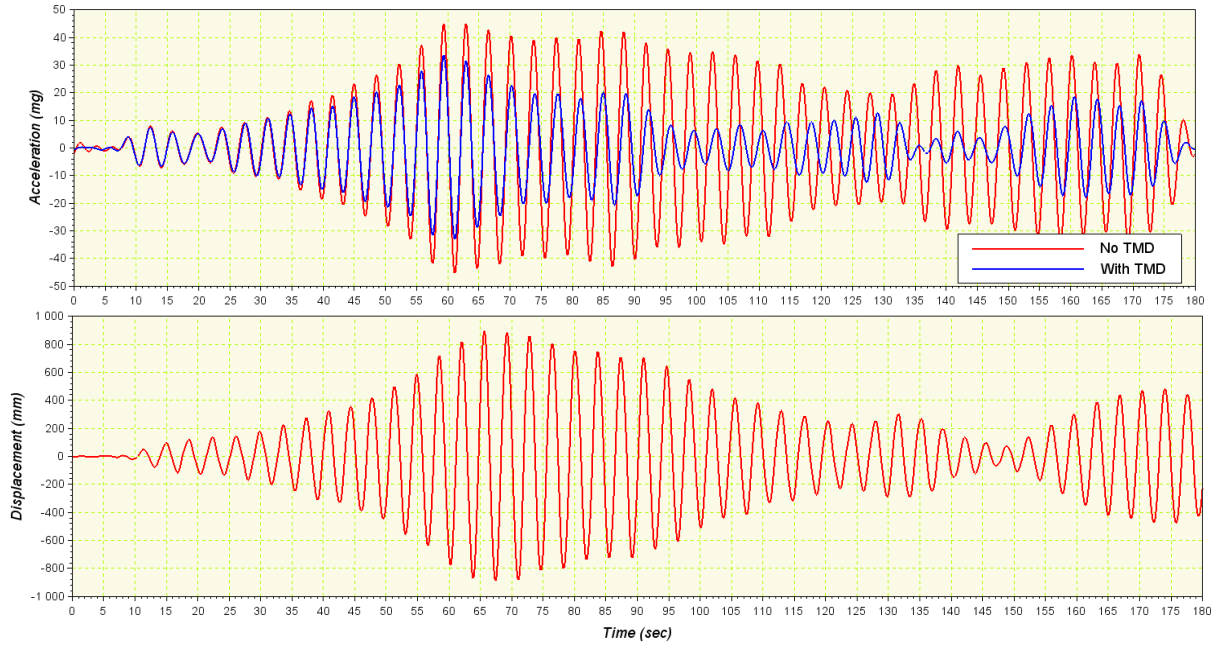

Figure 22 A-Frame Acceleration (Top) and Relative TMD Displacement (Bottom), Runs 63 and 64

The acceleration responses shown in Figure 21 and Figure 22 are low-pass filtered to exclude response at frequencies greater than 0.4 Hz to exclude contributions from frequencies that are higher than the 0.28-Hz sway mode frequency the TMDs are tuned to mitigate. The peak responses are summarized in Table 5 for storm winds applied normal to the Wheel and parallel to the Wheel. The A-Frame accelerations in parentheses are

the unfiltered values. The maximum response in the Y- and X-Directions do not act simultaneously. The X-Direction A-Frame acceleration is filtered to exclude frequencies above 1.0 Hz. The maximum horizontal-acting force exerted by the each TMD on the A-Frame is determined from the maximum TMD acceleration times the active TMD mass in that direction. Alternatively, the TMD force can be obtained from the product of the TMD displacement and the TMD spring stiffness acting in the same direction (assuming the relative velocity is zero). The forces reported in Table 5 do not include the vertical-acting overturning forces produced by the vertical offset of the TMD mass relative to the base nor the quasi-static shift in weight as the TMD mass moves from its equilibrium position through its sway range.

Table 5 Summary of TMD Motion for Worst-Case Storm Event

Response	Y-Direction (Normal)	X-Direction (Parallel)
Filtered A-Frame Acceleration (no TMDs)	51.1 mg (81.4 mg)	41.5 mg (45.6 mg)
Filtered A-Frame Acceleration (with TMDs)	31.2 mg (52.0 mg)	21.5 mg (24.7 mg)
Maximum TMD Displacement	950 mm	40 mm
Maximum TMD Acceleration	300 mg	85 mg
TMD Force on A-Frame (horizontal plane)	83.9 kN	20.2 kN

5.6 GUST-EFFECT FACTOR

The ASCE 7 wind load analysis procedure distinguishes between "rigid" and "dynamically sensitive" structures for the purpose of defining the wind loads that act on a structure. The gust effect factor, G, accounts for the size of the structure and its dynamic sensitivity. Larger structures are less susceptible to highly correlated pressure fluctuations because the scale of the pressure fluctuation is smaller than the structure and G is reduced accordingly. ASCE also defines a gust-effect factor for flexible structures, G_f, for cases where the wind-induced motion of a structure can be magnified by the structure's dynamics characteristics. Hence, G is the gust-effect factor for "rigid" structures (*i.e.*, not accounting for dynamic characteristics of the structure). ASCE 7-10 defines the rigid and flexible gust effect factors, respectively, as

$$G = 0.925\left(\frac{1+1.7I_{\bar{z}}g_Q Q}{1+1.7g_v I_{\bar{z}}}\right), \qquad G_f = 0.925\left(\frac{1+1.7I_{\bar{z}}\sqrt{g_Q^2 Q^2 + g_R^2 R^2}}{1+1.7g_v I_{\bar{z}}}\right), \tag{8}$$

where R is the resonant response factor and g_R is the peak factor for resonant response. Their product accounts for the dynamic sensitivity of the structure in the expression for G_f and ASCE 7 provides relatively simple formulas for their calculation for "typical" building-like structures. An alternative, but rational, approach for defining G_f based on the dynamics analyses performed for this study is defined in this section for the more unusual-shaped and more dynamically sensitive Wheel.

The basic ASCE 7 design wind force has the form:

$$F = q_z \begin{Bmatrix} G \\ G_f \end{Bmatrix} C_f A_f \,, \tag{9}$$

where q_z is the velocity pressure, C_f is the wind force coefficient, and A_f is the projected area of the structure normal to the wind. Since $G_f > G$, the applied force is higher for a dynamically-sensitive structure to account for inertia forces in the static analysis.

A slightly modified approach is adopted here, where the wind force is re-defined per

$$F = q_z K_f G C_f A_f, \qquad G_f = K_f G \tag{10}$$

The wind-induced system of forces, F, computed using G with no K_f accounts for the maximum response (displacement, shear force, bending moment, *etc.*) with no contribution from the motion of the structure (*i.e.*, no inertia forces). The system of forces computed using G_f accounts for the maximum system response including the inertia forces. For a rigid structure, the two responses are equal. The Wheel is not rigid, so an alternative gust effect factor for this dynamically sensitive structure is determined from the ratio, K_f, of the maximum response including the dynamics effects to the maximum response excluding the dynamics. The gust effect factor for rigid structures may be computed per ASCE 7. The resulting forces, F, or G used in a static analysis may then be scaled by K_f to obtain the wind-induced forces that account for the inertia effects.

The dynamics analyses performed for this study are used to determine appropriate and conservative values for K_f. The challenge with this approach is defining the "dynamic" response of the structure. A representation of the dynamic response of a single-degree-of-freedom (SDOF) structure is plotted in Figure 23. The total response of the system is divided into "static," "quasi-static," and "dynamic" portions, depending upon the excitation frequency relative to the fundamental resonance frequency of the system. The "static" and "quasi-static" responses, by definition, do not include significant contribution from the dynamic effects.

The resonance frequency, f_n, and critical damping ratio of the system represented in Figure 23 are 0.28 Hz and 0.5%, respectively to match the Y-Direction sway mode of the Wheel under storm conditions. The red line represents the ratio of the dynamic steady-state response of the SDOF system to the static response as a constant-amplitude harmonic applied force is swept from 0.01 Hz to 1 Hz. The static response corresponds to an excitation frequency of 0 Hz. For the purposes of this analysis, the quasi-static response frequency range is defined where the dynamic response magnitude is within 10% of the static response, and the dynamic response frequency range is defined for higher frequencies. The dynamic response is within 10% of the static force out to a frequency of $f_n/4$, or about 0.07 Hz. In other words, the dynamic response of the system is essentially equal to its static response for excitation frequencies below 0.07 Hz.

The wind force time histories applied to the Wheel include excitation frequencies from 0 Hz to 10 Hz. The Fourier series representation of those forces employed in this study effectively limits the upper frequency to 4 Hz. The critical point of interest here is that the response of the structure for wind force excitation frequencies lower than 0.07 Hz is no different from the static response according to Figure 23. Hence, wind force variation with frequencies below 0.07 Hz is accounted for by the static response of the structure. The dynamic response is obtained by performing a dynamics analysis with wind force time histories where the frequency content below 0.07 Hz is excluded. For example, the total raw wind force time history on the rim at $\phi = 0°$ is plotted in the top of Figure 24 along with the quasi-static (0 Hz < frequencies < 0.07 Hz) component. The remaining dynamic component of the wind force time history is obtained by subtracting the quasi-static force from the raw time history and is plotted in the bottom of Figure 24 for this location on the wheel.

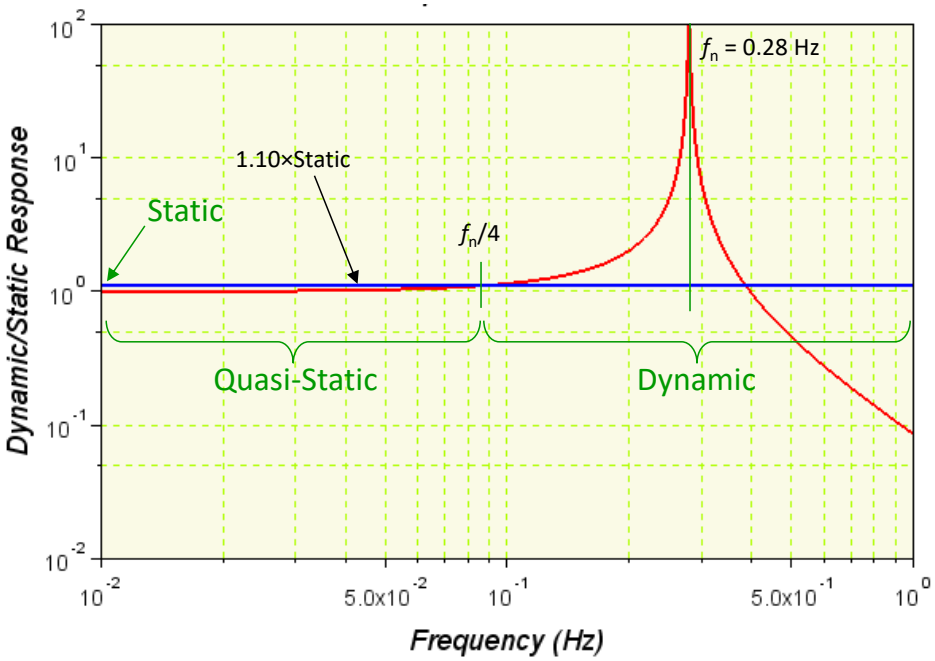

Figure 23 Quasi-Static and Dynamic Response of an SDOF System

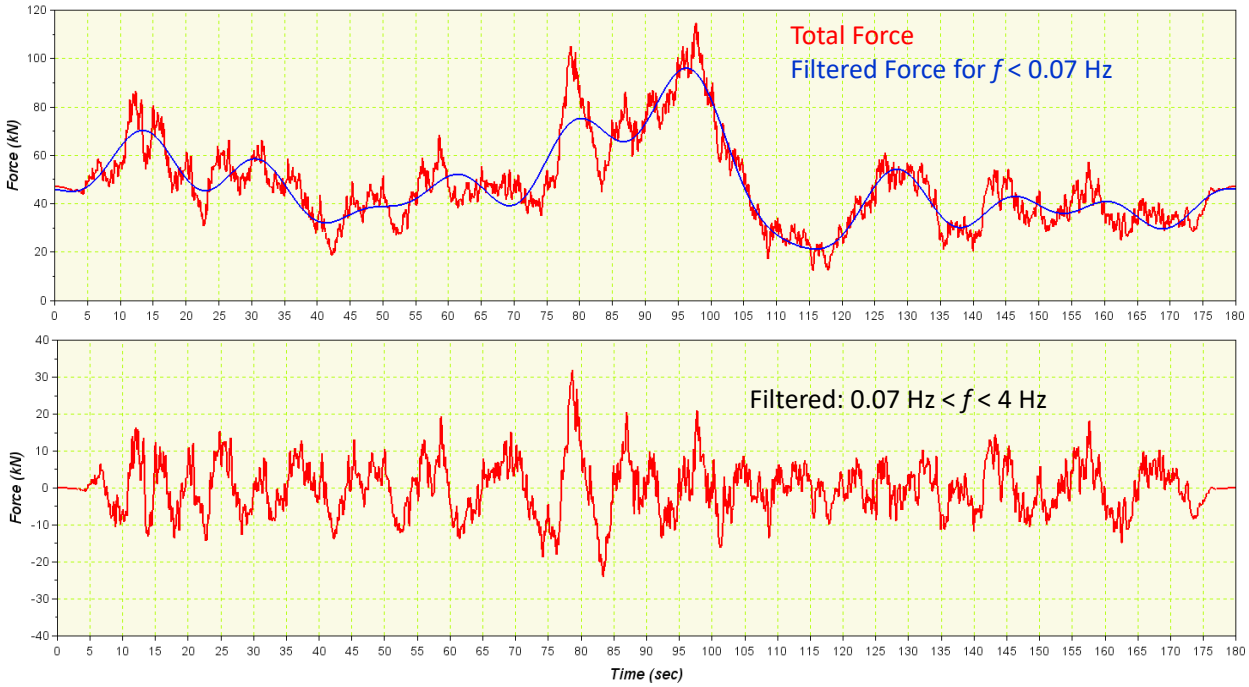

Figure 24 Total and Static Wind Force (Top) and Dynamic Wind Force (Bottom), ϕ = 0°

Filtered wind force time histories for each location on the structure are computed and applied to the Dynamics model of the Wheel. A static analysis is performed for the mean forces (f = 0 Hz). Dynamics analyses are performed for the quasi-static force time history (0 Hz < f < 0.07 Hz) and the dynamic time history (0.07 Hz < f <

4 Hz). Member forces and displacements at critical locations are then used to determine the gust-effect factor ratio per

$$K_f = \frac{G_f}{G} = \frac{R_D + R_S + R_{QS}}{R_S + R_{QS}}, \tag{11}$$

where R_S is the static response, R_{QS} is the quasi-static response, and R_D is the dynamic response. In this context, the "response" may be a force or bending moment in a structural member or a displacement at a location of interest. The gust-effect factor ratio is the ratio of the total response (including the dynamics component) to the static response (including the quasi-static component). Note that the maximum value attained by the numerator does not necessarily occur at the same time as the maximum value attained by the denominator. If the dynamics contribution is negligible, then $K_f \approx 1$. A plot of the rim displacement-based K_f is provided in Figure 25. A summary of gust effect factor ratios computed based on Equation (11) for critical responses is provided in Table 6.

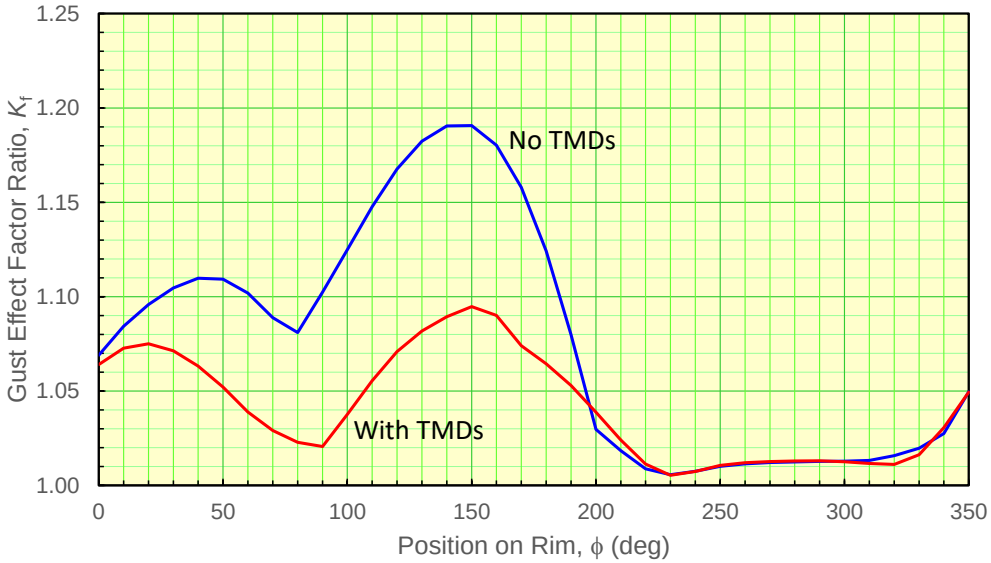

Figure 25 Gust Effect Factor for Rim Displacement

Table 6 Summary of Gust Effect Factor Ratios, K_f

Response	No TMDs	with TMDs
Rim Deflection	< 1.20	< 1.10
A-Frame Leg Axial Force	1.77	1.52
A-Frame Leg Shear Force	1.29	1.23
A-Frame Leg Bending Moment	1.33	1.24

Design forces and serviceability displacements for the Wheel may be determined using a traditional static analysis with ASCE-7-prescribed loads and a gust effect factor for a "rigid" structure. Ultimate strength design wind forces should be multiplied by the appropriate gust effect factor ratio to account for the

dynamic sensitivity of the Wheel. Wind-induced displacements required for serviceability should be multiplied by 1.2 (no TMDs) or 1.1 (with TMDs) to account for the dynamic effects.

5.7 STRUCTURAL MEMBER DESIGN WIND FORCE COMPARISON

The Wheel's structural design is based on static wind loads estimated to represent the 100-year wind load and the flexible structure effects are accounted for via the elevated gust effect factor for flexible structures. The dynamics analyses performed as outlined in this report, based on the wind field study force time histories, provide an independent source of wind-induced design loads that directly include the flexible structure dynamic magnification discussed in Section 5.6. A direct comparison of the 100-year static and dynamic design forces for representative structural members shown in Table 7.

The forces for the cable, rim/diagonal, rim/horizontal, and rim/chord members are taken from three representative locations around the perimeter: ϕ = 0°, 90°, and 270°. A positive axial force implies tension and a negative force implies compression. The bending moment in the member is included when significant and represents the total moment computed from the vector sum of the two orthogonal components. Wind-induced forces are included for the Wheel with and without the TMDs in the A-Frame. The TMDs provide structural load mitigation for the A-Frame legs, spindle, and cables, but provide essentially no mitigation for the rim members.

Table 7 Comparison of Service Wind-Induced Forces in Typical Structural Members

Member	Component	100-year	Dynamic No TMDs		Dynamic With TMDs	
		Static	Min	Max	Min	Max
Cables	Axial (kN)	-210 Min 670 Max	-120	400	-115	350
Spindle	Moment (kN·m)	±86,600		60,000		51,280
Rim Diagonal	Axial (kN)	±350	-310	250	-310	250
Rim Horizontal	Axial (kN)	±170	-75	90	-75	90
	Moment (kN·m)	±157		132		131
Rim Chord	Axial (kN)	±1,870	-1,420	1,495	-1,420	1,415
	Moment (kN·m)	±850		590		577
A-Frame Leg	Axial (kN)	±11,800	-9,650	9,305	-8,913	8,500
	Moment (kN·m)	±94,700		62,000		59,630

The wind-induced forces used by the EOR in the design of the Wheel are higher than those obtained from the structural dynamics analyses. The structural dynamics assessment provides the most realistic wind forces (obtained from wind tunnel tests) and the most accurate assessment of the dynamic magnification provided by the structural modes. The structural design of the Wheel is conservative.

6. CONCLUSIONS AND RECOMMENDATIONS

The primary modes of the Wheel structure responsible for the acceleration normal to the plane of the Wheel (Y-Direction) are the sway mode at 0.23 Hz, the torsion mode at 0.25 Hz, and the tilt mode at 0.38 Hz. The structural model indicates that the sway and tilt mode resonance frequencies increase to 0.28 Hz and 0.44 Hz, respectively, when the sustained wind forces are sufficiently high to push the Wheel against the drive structure. The primary structural mode responsible for the acceleration response parallel to the Wheel (X-Direction) is the X-Direction sway mode at 0.74 Hz.

The wind-induced dynamic response of the Wheel is much higher in the Y-Direction than the X-Direction; however, structural dynamics analyses indicate there are no concerns for occupant comfort. The acceleration environment at the occupant capsules easily satisfies the ISO 2631 Comfort criterion. In addition, peak accelerations in the capsules are expected to be less than 16 mg during operation.

The primary structural design loads are magnified by the dynamics characteristics of the Wheel structure. The A-Frame axial force can be about 1.8 times higher than the static response with the dynamic contribution with no TMDs. The A-Frame leg shear force and bending moment can be about 1.3 times higher than the corresponding static force and moment with no TMDs. The wind-induced forces in critical structural members obtained from these structural dynamics analyses using wind tunnel-derived forces are lower than those obtained from ASCE 7 and used in the design the Wheel. The structural design is conservative.

The proposed A-Frame-mounted TMDs reduce the highest occupant-perceived accelerations by 15% to 35%, depending upon the nature of the wind force variation with time and location on the rim. The TMDs also provide structural load mitigation for the A-Frame legs providing a 20% reduction in the maximum dynamic forces and moments in these members. Improved performance is possible by increasing the TMD mass (two 28.5-t TMDs are assumed in this study). The TMDs are not be required to achieve structural performance and/or occupant comfort objectives; however, the TMDs will provide reduced structural loads and increased occupant comfort.

There are several design and dynamics testing challenges that must be addressed for a successful implementation of the proposed TMDs. First, the modal analyses indicated that the Y-Direction sway mode could fall at 0.23 Hz for low-speed winds that govern occupant comfort or at 0.28 Hz for higher-speed winds that govern the structural design forces. A traditional TMD tuned to enhance the damping in the 0.28-Hz sway mode will not have a significant effect on the 0.23-Hz mode. In other words, a traditional TMD provides structural load mitigation or increases occupant comfort, but not both.

The two wind-speed-dependent Y-Direction sway mode resonance frequencies may be an artifact of the structural dynamics model developed for this study. It is understood that dynamics tests of the as-built Wheel structure are required to determine the actual resonance frequencies so that the (already installed) TMDs can be properly tuned. Simple measurements of the acceleration near the top of the A-Frame as its sways in response to typical low-level winds are sufficient to confirm the low-level resonance frequency but cannot provide the high-wind resonance frequency. Dynamics tests must be performed with the wheel “pushed” against the drive mechanism to reproduce the condition responsible for the higher 0.28-Hz resonance frequency.

The relative motion of the TMD mass in the X-Direction is only 40 mm when exposed to storm-level winds; however, the TMD displacement in the Y-Direction can be quite large. Structural load mitigation is only possible when the TMD mass is permitted to move through its full range of motion without contacting the hard stops. Extreme displacements of about 950 mm are predicted in the Y-Direction; however, this displacement is a maximum-observed displacement in 10 hours of a simulated force time history representing a worst-case storm

event. There is insufficient information available with specifics on the proposed TMD design to determine if a relative displacement of 950 mm can be accommodated where the TMDs are expected to be located in the A-Frame. It is also true that this relative displacement is highly improbable over the lifetime of the Wheel. A probabilistic study can be performed to develop the relationship between the relative TMD displacement and the probability of occurrence over the Wheel's lifetime and would form the basis for establishing the placement of the hard stops (*i.e.*, definition of the free motion length).

A preliminary assessment of the maximum lateral force imparted to the A-Frame as the TMD moves back and forth under worst-case storm conditions is 84 kN, but this estimate does not include the uplift forces created by the vertical offset of the TMD mass from the supporting A-Frame structural members. More significantly, the high forces that will result when the TMD mass impacts the hard stops cannot be evaluated until the hard stop locations and the stiffness and damping characteristics of the hard stops are provided by the TMD design agent. A more complete evaluation of these forces will be provided in a follow-up memorandum as more information about the TMD design is made available.

7. APPENDICES

Additional supporting information associated with this study is presented in this section for reference.

7.1 WORST-CASE CONDITIONS FOR REV0 DYNAMICS MODEL

The simplified 5-DOF model discussed in Section 5.2 is adjusted such that the Y-Direction sway mode has a resonance frequency of 0.23 Hz to match the EOR's initial stiffness model and the rev0 linearized Dynamics model. The simplified model is then used to determine the acceleration response at the rim and the TMD displacement for the 10 1-hour-long wind force time histories that comprise Case 1. The worst case 3-minute-long periods are summarized in Table 8.

Table 8 Summary of 5-DOF Simulation Peak Results (f_Y = 0.23 Hz)

Sim	Wind Force Case: 20 m/s @ 40° rel. North (Case 1)					
	Accel	Time	$Disp_{TMD}$	Time	$Force_{TMD}$	Time
1	15.1 mg	40.7 min	350 mm	36.7 min	20.9 kN	36.7 min
2	15.1 mg	26.4 min	256 mm	26.3 min	15.3 kN	26.3 min
3	18.2 mg	9.6 min	260 mm	40.8 min	15.5 kN	40.8 min
4	16.5 mg	34.4 min	329 mm	34.6 min	19.6 kN	34.6 min
5	19.8 mg	8.64 min	314 mm	0.6 min	18.7 kN	0.6 min
6	15.9 mg	36.4 min	300 mm	3.7 min	17.9 kN	3.7 min
7	16.7 mg	21.8 min	325 mm	13.8 min	19.4 kN	13.8 min
8	14.8 mg	33.7 min	313 mm	14.7 min	18.7 kN	14.7 min
9	16.3 mg	13.1 min	313 mm	14.7 min	18.7 kN	14.7 min
10	17.6 mg	34.8 min	318 mm	7.1 min	19.0 kN	7.1 min

7.2 DYNAMICS ANALYSIS RUN MATRIX

Likely worst periods for rim acceleration and TMD displacement in the 10-hour-long wind force time history files are identified using the simplified 5-DOF model as discussed in Section 5.2. The worst case 3-minute-long periods are summarized in Table 3 and Table 8. The three maximum peak conditions for acceleration and TMD displacement are shaded in the two tables. Structural dynamics analyses are performed for these periods with the various models. Each analysis is summarized in Table 9 including the model used, the wind force Case number (Case 1 = 40° relative North at 20 m/s, Case 3 = 40° relative North at 43.8 m/s), the Simulation number (1 through 10), wind direction (i.e., the oblique angle measured relative to Wheel's axis of rotation), the peak acceleration on the Wheel rim ("peak g") in mg, the maximum displacement of the TMD mass relative to A-Frame, the maximum absolute acceleration of the TMD, and the percent reduction in peak rim acceleration provided by the TMD.

Table 9 Summary Structural Dynamics Analyses

Run	Model	Case	Simulation	Oblique	T (start)	T (final)	Directory	Date	Peak mg	TMD mm	TMD mg	TMD %
1	Wheel Dynamics rev1 NO TMD	1	5	0	7	10	Run 01	5/17/2016	24.7			
2	Wheel Dynamics rev1 NO TMD	1	5	80	7	10	Run 02	5/17/2016	13.0			
3	Wheel Dynamics rev1 TMD	1	5	0	7	10	Run 03	5/17/2016	23.0	85	27	0.07
4	Wheel Dynamics rev1 RIM TMD	1	5	0	7	10	Run 04	5/18/2016	21.6			0.13
5	Wheel Dynamics rev1 NO TMD	1	9	0	51	54	Run 05	5/18/2016	31.0			
6	Wheel Dynamics rev1 TMD	1	9	0	51	54	Run 06	5/18/2016	22.6	154	48	0.27
7	Wheel Dynamics rev1 RIM TMD	1	9	0	51	54	Run 07	5/18/2016	19.3			0.38
8	Wheel Dynamics rev1 NO TMD	1	7	0	38.5	41.5	Run 08	5/19/2016	21.7			
9	Wheel Dynamics rev1 TMD	1	7	0	38.5	41.5	Run 09	5/19/2016	22.0	97	31	-0.01
10	Wheel Dynamics rev1 RIM TMD	1	7	0	38.5	41.5	Run 10	5/20/2016	18.4			0.15
11	Wheel Dynamics rev1 NO TMD	1	1	0	23	26	Run 11	5/20/2016	33.7			
12	Wheel Dynamics rev1 TMD	1	1	0	23	26	Run 12	5/20/2016	26.7	164	52	0.21
13	Wheel Dynamics rev1 RIM TMD	1	1	0	23	26	Run 13	5/20/2016	20.4			0.39
14	Wheel Dynamics rev1 NO TMD	1	10	0	31	34	Run 14	5/20/2016	23.5			
15	Wheel Dynamics rev1 TMD	1	10	0	31	34	Run 15	5/20/2016	23.1	96	30	0.02
16	Wheel Dynamics rev1 RIM TMD	1	10	0	31	34	Run 16	5/20/2016	21.8			0.07
17	Wheel Dynamics rev1 NO TMD	1	4	0	14	17	Run 17	5/20/2016	24.7			
18	Wheel Dynamics rev1 TMD	1	4	0	14	17	Run 18	5/20/2016	23.0	132	42	0.07
19	Wheel Dynamics rev1 RIM TMD	1	4	0	14	17	Run 19	5/21/2016	19.2			0.22
20	Wheel Dynamics rev1 NO TMD	1	9	90	51	54	Run 20	5/21/2016	13.7			
21	Wheel Dynamics rev1 NO TMD	1	1	90	23	26	Run 21	5/21/2016	13.2			
22	Wheel Dynamics rev1 TMD	1	9	90	51	54	Run 22	5/21/2016	12.2	7	15	0.11
23	Wheel Dynamics rev0 NO TMD	1	1	0	35	38	Run 23	5/23/2016	35.5			
24	Wheel Dynamics rev0 TMD	1	1	0	35	38	Run 24	5/24/2016	30.0	204	44	0.15
25	Wheel Dynamics rev0 NO TMD	1	3	0	8	11	Run 25	5/23/2016	23.0			
26	Wheel Dynamics rev0 TMD	1	3	0	8	11	Run 26	5/24/2016	23.7	109	23	-0.03
27	Wheel Dynamics rev0 NO TMD	1	4	0	33	36	Run 27	5/23/2016	24.7			
28	Wheel Dynamics rev0 TMD	1	4	0	33	36	Run 28	5/25/2016	24.3	132	28	0.02
29	Wheel Dynamics rev0 NO TMD	1	5	0	7	10	Run 29	5/23/2016	26.9			
30	Wheel Dynamics rev0 TMD	1	5	0	7	10	Run 30	5/25/2016	23.1	143	31	0.14
31	Wheel Dynamics rev0 NO TMD	1	7	0	12.5	15.5	Run 31	5/23/2016	31.8			
32	Wheel Dynamics rev0 TMD	1	7	0	12.5	15.5	Run 32	5/24/2016	22.1	254	54	0.31
33	Wheel Dynamics rev0 NO TMD	1	10	0	33.5	36.5	Run 33	5/23/2016	25.3			
34	Wheel Dynamics rev0 TMD	1	10	0	33.5	36.5	Run 34	5/25/2016	21.7	157	34	0.14
35	Wheel Dynamics rev0 NO TMD	1	6	0	26	29	Run 35	5/26/2016	30.7			
36	Wheel Dynamics rev0 TMD	1	6	0	26	29	Run 36	5/26/2016	25.9	184	39	0.16
37	Wheel Dynamics rev1 NO TMD	1	6	0	41	44	Run 37	5/27/2016	24.7			
38	(not run)											
39	(not run)											
40	Wheel Dynamics rev1 NO TMD	1	8	0	4.5	7.5	Run 40	5/27/2016	33.3			
41	Wheel Dynamics rev1 TMD	1	8	0	4.5	7.5	Run 41	5/30/2016	25.5	113	36	0.23
42	Wheel Dynamics rev1 RIM TMD	1	8	0	4.5	7.5	Run 42	5/30/2016	20.4			0.39
43	Wheel Dynamics rev1 NO TMD	1	7	0	32	35	Run 43	5/27/2016	31.7			
44	Wheel Dynamics rev1 TMD	1	7	0	32	35	Run 44	5/28/2016	20.9	100	32	0.34
45	Wheel Dynamics rev1 RIM TMD	1	7	0	32	35	Run 45	5/28/2016	19.6			0.38
46	Wheel Dynamics rev1 NO TMD	1	2	0	1.5	4.5	Run 46	5/28/2016	34.5			
47	Wheel Dynamics rev1 TMD	1	2	0	1.5	4.5	Run 47	5/28/2016	28.9	158	50	0.16
48	Wheel Dynamics rev1 RIM TMD	1	2	0	1.5	4.5	Run 48	5/28/2016	24.0			0.30
49	Wheel Dynamics rev0 NO TMD	1	10	0	6	9	Run 49	5/28/2016	30.0			
50	Wheel Dynamics rev0 TMD	1	10	0	6	9	Run 50	5/28/2016	24.3	223	48	0.19
51	Wheel Dynamics rev0 NO TMD	1	5	0	0	3	Run 51	5/29/2016	20.6			
52	Wheel Dynamics rev0 TMD	1	5	0	0	3	Run 52	5/29/2016	20.3	169	36	0.01
53	Wheel Dynamics rev0 NO TMD	1	1	90	35.5	38.5	Run 53	5/29/2016	14.4			
54	Wheel Dynamics rev0 TMD	1	1	90	35.5	38.5	Run 54	5/29/2016	11.1	7	16	0.23
55	Wheel Dynamics rev0 NO TMD	1	5	90	5.5	8.5	Run 55	5/29/2016	13.3			
56	Wheel Dynamics rev0 TMD	1	5	90	5.5	8.5	Run 56	5/29/2016	12.1	9	19	0.09
57	Wheel Dynamics rev0 NO TMD	1	7	90	7.5	10.5	Run 57	5/29/2016	11.5			
58	Wheel Dynamics rev0 TMD	1	7	90	7.5	10.5	Run 58	5/29/2016	10.1	7	16	0.12
59	Wheel Dynamics rev0 RIM TMD	1	1	0	35	38	Run 59	5/30/2016	27.9			0.21
60	Wheel Dynamics rev0 RIM TMD	1	7	0	12.5	15.5	Run 60	5/30/2016	17.7			0.44
61	Wheel Dynamics rev0 RIM TMD	1	6	0	26	29	Run 61	5/30/2016	20.6			0.33
62	Wheel Dynamics rev0 OPT RIM TMD	1	1	0	35	38	Run 62	5/31/2016	27.2			
63	Wheel Dynamics rev1 NO TMD	3	2	0	1.5	4.5	Run 63	6/1/2016	196.5			
64	Wheel Dynamics rev1 TMD	3	2	0	1.5	4.5	Run 64	6/1/2016	165.9	894	282	0.16
65	Wheel Dynamics rev1 NO TMD	3	1	0	23	26	Run 65	6/2/2016	188.2			
66	Wheel Dynamics rev1 TMD	3	1	0	23	26	Run 66	6/2/2016	150.0	951	300	0.20
67	Wheel Dynamics rev1 NO TMD	3	8	0	4.5	7.5	Run 67	6/2/2016	189.8			
68	Wheel Dynamics rev1 TMD	3	8	0	4.5	7.5	Run 68	6/2/2016	142.7	624	197	0.25
69	Wheel Dynamics rev0 NO TMD	3	1	90	35.5	38.5	Run 69	6/4/2016	77.5			
70	Wheel Dynamics rev0 TMD	3	1	90	35.5	38.5	Run 70	6/4/2016	60.6	39	85	0.22